UMN-TH-3135/13

Prepared for submission to JCAP

Signatures of anisotropic sources in the squeezed-limit bispectrum of the cosmic microwave background

Maresuke Shiraishi,[a] **Eiichiro Komatsu,**[b,c,d] **Marco Peloso,**[e,f] **and Neil Barnaby**[g]

[a]Department of Physics and Astrophysics, Nagoya University, Nagoya, Aichi 464-8602, Japan
[b]Max-Planck-Institut für Astrophysik, Karl-Schwarzschild Str. 1, 85741 Garching, Germany
[c]Kavli Institute for the Physics and Mathematics of the Universe, Todai Institutes for Advanced Study, the University of Tokyo, Kashiwa, Japan 277-8583 (Kavli IPMU, WPI)
[d]Texas Cosmology Center and the Department of Astronomy, The University of Texas at Austin, 1 University Station, C1400, Austin, TX 78712, USA
[e]School of Physics and Astronomy, University of Minnesota, Minneapolis 55455, USA
[f]INFN, Sezione di Padova, via Marzolo 8, I-35131, Padova, Italy
[g]Department of Applied Mathematics and Theoretical Physics, Center for Mathematical Sciences, Wilberforce Road, Cambridge, CB3 0WA, UK

Abstract. The bispectrum of primordial curvature perturbations in the squeezed configuration, in which one wavenumber, k_3, is much smaller than the other two, $k_3 \ll k_1 \approx k_2$, plays a special role in constraining the physics of inflation. In this paper we study a new phenomenological signature in the squeezed-limit bispectrum: namely, the amplitude of the squeezed-limit bispectrum depends on an angle between $\mathbf{k}_1$ and $\mathbf{k}_3$ such that $B_\zeta(k_1, k_2, k_3) \to 2\sum_L c_L P_L(\hat{\mathbf{k}}_1 \cdot \hat{\mathbf{k}}_3) P_\zeta(k_1) P_\zeta(k_3)$, where P_L are the Legendre polynomials. While c_0 is related to the usual local-form $f_{\rm NL}$ parameter as $c_0 = 6f_{\rm NL}/5$, the higher-multipole coefficients, c_1, c_2, etc., have not been constrained by the data. Primordial curvature perturbations sourced by large-scale magnetic fields generate non-vanishing c_0, c_1, and c_2. Inflation models whose action contains a term like $I(\phi)^2F^2$ generate $c_2 = c_0/2$. A recently proposed "solid inflation" model generates $c_2 \gg c_0$. A cosmic-variance-limited experiment measuring temperature anisotropy of the cosmic microwave background up to $\ell_{\rm max} = 2000$ is able to measure these coefficients down to $\delta c_0 = 4.4$, $\delta c_1 = 61$, and $\delta c_2 = 13$ (68% CL). We also find that c_0 and c_1, and c_0 and c_2, are nearly uncorrelated. Measurements of these coefficients will open up a new window into the physics of inflation such as the existence of vector fields during inflation or non-trivial symmetry structure of inflaton fields. Finally, we show that the original form of the Suyama-Yamaguchi inequality does not apply to the case involving higher-spin fields, but a generalized form does.

Contents

1 Introduction

Convincing detection of the so-called "local-form" three-point correlation function (bispectrum) of primordial curvature perturbations from inflation would rule out all single-field inflation models [1, 2], provided that an initial quantum state of the curvature perturbation is in a preferred state called the Bunch-Davies state [3, 4] and that the curvature perturbation does not evolve outside the horizon due to a non-attractor solution [5, 6].[1]

The curvature perturbation, ζ, is defined as a trace part of space-space components of the metric perturbation, $\delta g_{ij} = a^2(t)e^{2\zeta}\delta_{ij}$, in a uniform density gauge. The bispectrum of ζ is defined as $\langle\zeta_{\mathbf{k}_1}\zeta_{\mathbf{k}_2}\zeta_{\mathbf{k}_3}\rangle = (2\pi)^3\delta^{(3)}(\mathbf{k}_1+\mathbf{k}_2+\mathbf{k}_3)\,B_\zeta(k_1,k_2,k_3)$, and the local-form bispectrum is defined as $B_\zeta(k_1,k_2,k_3) = \frac{6}{5}f_{\rm NL}\left[P_\zeta(k_1)P_\zeta(k_2)+P_\zeta(k_2)P_\zeta(k_3)+P_\zeta(k_3)P_\zeta(k_1)\right]$ (e.g., [7]), where $P_\zeta(k) \propto k^{n_s-4}$ is the power spectrum of the primordial curvature perturbation with $n_s = 0.96 \pm 0.01$ [8–10]. This means that the local-form bispectrum has the largest amplitude in the so-called squeezed configuration, in which the smallest wavenumber, k_3, is much smaller than the other two, i.e., $k_3 \ll k_1 \approx k_2$ [11]. In this limit the local-form bispectrum is given by $B_\zeta \to \frac{12}{5}f_{\rm NL}P_\zeta(k_1)P_\zeta(k_3)$, and all attractor single-field inflation models with a Bunch-Davies initial state give $f_{\rm NL} = \frac{5}{12}(1-n_s)$ [1, 12].

The current best limit on $f_{\rm NL}$ is $f_{\rm NL} = 37 \pm 20$ (68% CL), which was obtained from the *Wilkinson Microwave Anisotropy Probe* (*WMAP*) 9-year data with the expected ISW-lensing bias removed [13]. The forthcoming *Planck* data are expected to reduce the error bar by a factor of four [7].

[1] Also see workshop summaries of "Critical Tests of Inflation Using Non-Gaussianity" in http://www.mpa-garching.mpg.de/~komatsu/meetings/ng2012/.

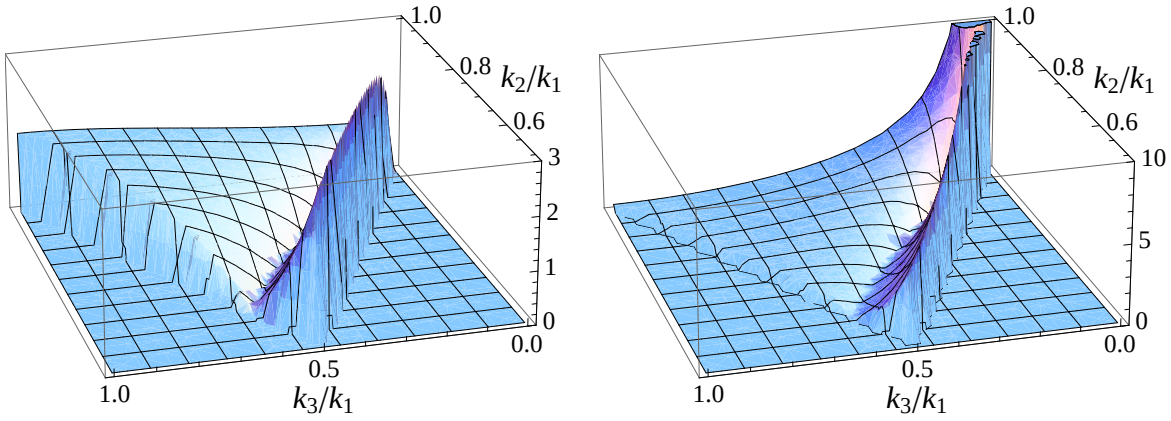

Figure 1. Absolute values of the shape function of $L = 1$, $(k_1k_2k_3)^2S_1$ (left panel), and that of $L = 2$, $(k_1k_2k_3)^2S_2$ (right panel). We restrict the plot range to $k_3 \leq k_2 \leq k_1$ and $|k_1 - k_2| \leq k_3 \leq k_1 + k_2$ for symmetry and the triangular condition. The shape of $L = 2$ peaks at the squeezed configuration, $k_3/k_1 \ll 1$ and $k_2/k_1 \approx 1$, whereas the shape of $L = 1$ is suppressed at the squeezed configuration.

If the *Planck* collaboration finds evidence for $f_{\rm NL}$, or the lack thereof, what is next? Measuring the local-form four-point function (trispectrum) [14, 15] to check the so-called Suyama-Yamaguchi inequality between the amplitude of the local-form trispectrum and $f_{\rm NL}$, i.e., $\tau_{\rm NL} \geq (6f_{\rm NL}/5)^2$ [16–21], would be an important next step to understand the nature of sources of non-Gaussianity (or the absence thereof). We shall discuss the Suyama-Yamaguchi inequality within the context of higher-spin fields in Sec. 4.

Can we learn more about sources of non-Gaussianity by further scrutinizing the behavior of the bispectrum in the squeezed configuration? The answer is yes, and this is the main goal of this paper. Namely, in this paper, we shall investigate phenomenological consequences of the following new parametrization of the bispectrum of primordial curvature perturbations:

$$B_\zeta(k_1, k_2, k_3) = \sum_L c_L P_L(\hat{\mathbf{k}}_1 \cdot \hat{\mathbf{k}}_2) P_\zeta(k_1) P_\zeta(k_2) + (2 \text{ perm}) \ , \tag{1.1}$$

where $P_L(\mu)$ is the usual Legendre polynomials, i.e., $P_0(\mu) = 1$, $P_1(\mu) = \mu$, and $P_2(\mu) = \frac{1}{2}(3\mu^2 - 1)$. Here, c_0 is equal to $6f_{\rm NL}/5$.[2]

Why consider c_L with $L \geq 1$? These coefficients appear to be sensitive to the existence of vector fields. For example, curvature perturbations sourced by primordial magnetic fields produce non-zero c_1 and c_2 [22, 23]. Curvature perturbations sourced by a $\frac{1}{4}I(\phi)^2F^2$ term in Lagrangian produce $c_2 = c_0/2$ [24, 25]. These coefficients are also sensitive to the existence of a non-trivial realization of SO(3) rotational symmetry during inflation: a recently proposed "solid inflation" model produces $c_2 \gg c_0$ [26]. While the second-order effects in General Relativity also induce non-trivial angular dependence in the bispectrum, it disappears in the squeezed limit [27], and thus will not be considered in this paper.

While we assume that the coefficients, c_L, do not depend on wavenumbers, it is entirely possible that they do. There are various ways in which $c_0 = 6f_{\rm NL}/5$ depends on wavenumbers

[2]Note that, due to symmetry, the c_1 term as well as any odd L terms vanish in the exact squeezed limit, i.e., $\lim_{k_3 \to 0} B_\zeta(k_1, k_2, k_3) = 2[c_0 + c_2P_2(\mu_{13}) + c_4P_4(\mu_{13}) + \dots]P_\zeta(k_1)P_\zeta(k_3)$, where $\mu_{13} \equiv \hat{\mathbf{k}}_1 \cdot \hat{\mathbf{k}}_3$. As a result, when we analyze the CMB data, the error bar of c_1 is much bigger than the error bars of c_0 and c_2, as we shall show in Sec 3.3. On the other hand, the error bars of c_0 and c_2 are expected to be comparable: we shall show that they are related by $\delta c_2 \approx 3\delta c_0$ in Sec 3.3.

[3, 4, 28–32]. Particularly interesting possibilities are strongly infrared-divergent c_1 and c_2, which can naturally give rise to dipoler (i.e., hemispherical) and quadrupolar modulations, respectively, of the observed power spectrum in our sky [33].

In Sec. 2, we shall briefly review these three scenarios to motivate our choice of parametrization given in Eq. (1.1). Specifically, we review non-Gaussianities generated from: (1) large-scale magnetic fields after inflation in Sec 2.1; (2) a vector field coupled to the inflaton field, ϕ, through a dilaton-like coupling $I^2(\phi)F^2$ in Sec 2.2; and (3) solid inflation, in which the inflaton field is a part of a vector multiplet, $\left\{\phi^1, \phi^2, \phi^3\right\}$, in Sec 2.3.

What do the shapes of $L = 1$ and $L = 2$ terms look like? Using the triangular condition of three wavevectors, $\mathbf{k}_1 + \mathbf{k}_2 + \mathbf{k}_3 = 0$, the cosine between wavenumbers can be written as, e.g., $\hat{\mathbf{k}}_1 \cdot \hat{\mathbf{k}}_2 = (k_3^2 - k_1^2 - k_2^2)/(2k_1k_2)$. Then, for a scale-invariant power spectrum of ζ, $P_\zeta(k) = \frac{2\pi^2}{k^3}A_S$, Eq. (1.1) can be re-written as

$$B_\zeta(k_1, k_2, k_3) = (2\pi^2 A_S)^2 \sum_L c_L S_L(k_1, k_2, k_3) \ , \tag{1.2}$$

where

$$S_0(k_1, k_2, k_3) = \left(\frac{1}{k_1^3 k_2^3} + 2 \text{ perm}\right) \ , \tag{1.3}$$

$$S_1(k_1, k_2, k_3) = \left(\frac{k_1^2}{2k_2^4 k_3^4} + 2 \text{ perm}\right) - \left(\frac{1}{2k_1^4 k_2^2} + 5 \text{ perm}\right) \ , \tag{1.4}$$

$$\begin{aligned} S_2(k_1, k_2, k_3) = &\left(\frac{3k_1^4}{8k_2^5 k_3^5} + 2 \text{ perm}\right) - \left(\frac{3k_1^2}{4k_2^5 k_3^3} + 5 \text{ perm}\right) \\ &+ \left(\frac{3}{8k_1^5 k_2} + 5 \text{ perm}\right) + \left(\frac{1}{4k_1^3 k_2^3} + 2 \text{ perm}\right) \ . \end{aligned} \tag{1.5}$$

In Figure 1, we show the shape functions S_1 (left panel) and S_2 (right one). The right panel shows that the bispectrum for $L = 2$ peaks in the squeezed limit ($k_3 \ll k_1 \approx k_2$), whereas the left panel shows that the bispectrum for $L = 1$ is suppressed in the squeezed limit (also see footnote 2).

The rest of this paper is organized as follows. In Sec. 3, we derive both the full-sky and flat-sky formulae of the bispectrum of temperature anisotropies of the cosmic microwave background (CMB) induced by the angle-dependent bispectrum given in Eq. (1.1), and analyze their behaviors. We also estimate the error bars of c_L for $L = 0$, 1, and 2, expected for a cosmic-variance-limited CMB experiment measuring temperature anisotropy up to $\ell_{\rm max} = 2000$. In Sec. 4, we revisit the Suyama-Yamaguchi inequality within the context of higher-spin fields such as those discussed in this paper. We conclude in Sec. 5. In Appendix A, we discuss the precision of the flat-sky approximation. In Appendix B, we derive the CMB bispectrum in the Sachs–Wolfe limit (in which the temperature anisotropy is given by $\delta T/T = -\zeta/5$). In Appendix C, we present the full Fisher matrix for c_0, c_1, and c_2.

Throughout this paper, we adopt the following convention for Fourier transformation of an arbitrary function, $f(\mathbf{x})$: $f(\mathbf{x}) = \int \frac{d^3\mathbf{k}}{(2\pi)^3} f(\mathbf{k}) e^{i\mathbf{k}\cdot\mathbf{x}}$.

2 Theoretical motivation

2.1 Helical and non-helical magnetic fields

Astrophysical observations suggest the existence of magnetic fields on the order of 10^{-6} G in galaxies and cluster of galaxies [34–37]. There is also indirect evidence for the existence of

magnetic fields on the order of $10^{-20} - 10^{-14}$ G in the inter-galactic medium (IGM) [38–41].

There is yet no compelling model for how these vector fields can be generated during inflation, as the existing models suffer from strong backreaction or strong coupling problems [24, 42–46] (see the more detailed discussion in the next subsection). Here we simply assume that a magnetic field has been generated,[3] and study its impact on the primordial perturbations during the radiation era and recombination. In the next subsection, we discuss the additional signatures that take place if vector fields are coupled to the inflaton field.

A large amount of literature exist in the studies of effects of vector fields on CMB anisotropies and the large-scale structure of the universe. See, e.g., [47–60] for effects on the two-point correlation functions, and [22, 23, 61–67] for those on higher-order correlation functions.

Let us assume that super-horizon vector perturbations were produced during inflation, and they generated large-scale magnetic fields. The anisotropic stress of this magnetic field sources the growth of curvature perturbation via Einstein's field equations during the radiation era. However, after the decoupling of neutrinos at a few MeV, the magnetic anisotropic stress is compensated by the neutrino anisotropic stress, and the curvature perturbation on super-horizon scales becomes a constant. This constant curvature perturbation survives till the recombination epoch, and seeds additional CMB anisotropies. The solution of curvature perturbations on super-horizon scales is determined by the traceless projection of the magnetic anisotropic stress as [53]

$$\zeta_{\mathbf{k}} \approx 0.9 \ln\left(\frac{\tau_\nu}{\tau_B}\right)\left(\hat{k}^j\hat{k}_i - \frac{1}{3}\delta^j{}_i\right)\frac{1}{4\pi\rho_{\gamma,0}}\int\frac{d^3\mathbf{k}'}{(2\pi)^3}B^i(\mathbf{k}')B_j(\mathbf{k}-\mathbf{k}'), \tag{2.1}$$

where τ_B and τ_ν denote the conformal time of the generation of magnetic fields and that of the decoupling of neutrinos, respectively, and $\rho_{\gamma,0}$ is the present-day value of the photon energy density. This equation shows that, even under the assumption that the magnetic field itself is a Gaussian variable, the curvature perturbations become highly non-Gaussian.

Angular dependence of the power spectrum and bispectrum arises due to the spin-1 nature of magnetic fields. The magnetic field vector is transverse, $k^iB_i = 0$, and thus it is expanded using the spin-1 polarization vector, $e_i^{(\sigma)}(\hat{\mathbf{k}})$: $B_i(\mathbf{x}) = (2\pi)^{-3}\int d^3\mathbf{k}\; B_i(\mathbf{k})e^{i\mathbf{k}\cdot\mathbf{x}} = (2\pi)^{-3}\int d^3\mathbf{k}\;\sum_{\sigma=\pm1}B^\sigma(\mathbf{k})e_i^{(\sigma)}(\hat{\mathbf{k}})e^{i\mathbf{k}\cdot\mathbf{x}}$, where σ denotes two circular polarization states. Then, the power spectrum of magnetic fields can be decomposed into the "non-helical," $P_B(k)$, and "helical," $P_{\mathcal{B}}(k)$, components as [68]

$$\begin{aligned}\left\langle B_i(\mathbf{k})B_j(\mathbf{k}')\right\rangle &= \frac{(2\pi)^3}{2}\delta^{(3)}(\mathbf{k}+\mathbf{k}')\sum_{\sigma=\pm1}\left[P_B(k) - \sigma P_{\mathcal{B}}(k)\right]e_i^{(\sigma)}(\hat{\mathbf{k}})e_j^{(-\sigma)}(\hat{\mathbf{k}}) \\ &= \frac{(2\pi)^3}{2}\delta^{(3)}(\mathbf{k}+\mathbf{k}')\left[(\delta_{ij}-\hat{k}_i\hat{k}_j)P_B(k) + i\epsilon_{ijl}\hat{k}^lP_{\mathcal{B}}(k)\right],\end{aligned} \tag{2.2}$$

[3] While we use the term "magnetic field" and "electric field" here and in the next subsection, these fields are not necessarily the usual electromagnetic fields. For the discussion in this subsection, it is sufficient to have some vector field whose anisotropic stress decays as $T^i_j - \frac{1}{3}\delta^i_jT^k_k \propto a^{-4}$ on super-horizon scales. On the other hand, the anisotropic stress on super-horizon scales is constant during inflation (disregarding slow-roll corrections) for the case we discuss in the next subsection. The important feature of these models is that the anisotropic stress scales with a in the same way as the isotropic pressure dominating the universe: for the former case, it scales in the same way the radiation pressure does, and for the latter it scales in the same way the inflaton pressure does.

where ϵ_{ijl} is the antisymmetric tensor normalized as $\epsilon_{123} = 1$. These power spectra are defined as

$$\langle B^+(\mathbf{k})B^+(\mathbf{k}')\rangle + \langle B^-(\mathbf{k})B^-(\mathbf{k}')\rangle = (2\pi)^3 P_B(k)\delta^{(3)}(\mathbf{k}+\mathbf{k}'), \tag{2.3}$$

$$-\langle B^+(\mathbf{k})B^+(\mathbf{k}')\rangle + \langle B^-(\mathbf{k})B^-(\mathbf{k}')\rangle = (2\pi)^3 P_{\mathcal{B}}(k)\delta^{(3)}(\mathbf{k}+\mathbf{k}'). \tag{2.4}$$

Note that the overall sign of the definition of these spectra depends on the choice of the polarization vector. Here, we adopt the definition of Ref. [23].

Using these power spectra, one can write the angle dependence of the bispectrum of curvature perturbations as [23]

$$\begin{aligned} B_\zeta(\mathbf{k}_1,\mathbf{k}_2,\mathbf{k}_3) \propto\ & P_B(k_*)P_B(k_1)P_B(k_2)\left(\frac{1}{3}\mu_{12}^2+\mu_{23}^2+\mu_{31}^2-\frac{2}{3}-\mu_{12}\mu_{23}\mu_{31}\right) \\ & - P_B(k_*)P_{\mathcal{B}}(k_1)P_{\mathcal{B}}(k_2)\left(\mu_{23}\mu_{31}-\frac{1}{3}\mu_{12}\right) \\ & + (1\to 3,\ 2\to 1,\ 3\to 2) + (1\to 2,\ 2\to 3,\ 3\to 1)\ , \end{aligned} \tag{2.5}$$

where $\mu_{ab} \equiv \hat{\mathbf{k}}_a \cdot \hat{\mathbf{k}}_b$ and k_* denotes some pivot wavenumber.[4]

Eq. (2.5) clearly shows that helical and non-helical magnetic fields generate $L = 1$ and $L = 2$ angular dependence in the bispectrum of curvature perturbations. If the magnetic field was generated at a GUT scale, i.e., $\tau_\nu/\tau_B \approx 10^{17}$, with nearly scale-invariant spectra of P_B and $P_{\mathcal{B}}$, the Legendre coefficients in Eq. (1.1) are related to the amplitudes of non-helical and helical magnetic fields smoothed on 1 Mpc as [23]

$$c_0 \approx -2\times 10^{-4}\left(\frac{B_{1\mathrm{Mpc}}}{\mathrm{nG}}\right)^6, \quad c_1 \approx -0.9\left(\frac{B_{1\mathrm{Mpc}}}{\mathrm{nG}}\right)^2\left(\frac{\mathcal{B}_{1\mathrm{Mpc}}}{\mathrm{nG}}\right)^4, \quad c_2 \approx 14 c_0. \tag{2.6}$$

Therefore, if inflation creates $B_{1\mathrm{Mpc}} \sim 3\mathrm{nG}$ and $\mathcal{B}_{1\mathrm{Mpc}} \sim 1\mathrm{nG}$, which are consistent with the current observational limits, we may have negative and non-vanishing c_1 and c_2; namely, $c_1 \sim -8$ and $c_2 \sim -2$.

2.2 $I^2(\phi)F^2$ model

Vector fields with the standard Maxwell $-F^2/4$ kinetic term are not produced by the expansion of the universe and, if generated by some other source, they are rapidly diluted away. This poses a challenge to models of primordial magnetogenesis and of vector fields during inflation. Vector fields during inflation can result in broken statistical isotropy of the primordial perturbations, which will be probed by the forthcoming *Planck* data [70, 71].

Vector fields with a kinetic term given by

$$\mathcal{L} = -\frac{I^2(\phi)}{4}F^2\ , \tag{2.7}$$

can instead be produced during inflation if $I(t)$ has an appropriate time dependence [72]. It is convenient to define the "electric" and "magnetic" components

$$E_i = -\frac{I}{a^2}A_i'\ ,\quad B_i = \frac{I}{a^2}\epsilon_{ijk}\partial_j A_k\ , \tag{2.8}$$

[4]Note that parity-odd terms, which are proportional to $P_B^2 P_{\mathcal{B}}$ and $P_{\mathcal{B}}^3$, do not appear in Eq. (2.5), as ζ is a scalar. On the other hand, the bispectrum involving vector or tensor perturbations may contain parity-odd terms, which yield the CMB temperature auto-bispectrum with $\ell_1+\ell_2+\ell_3 = \mathrm{odd}$ [23, 69].

where the primes denote derivatives with respect to the conformal time, and a is the scale factor of the universe. In terms of these components, the physical energy density in the vector field assumes the conventional expression, $\rho_A = \frac{|\mathbf{E}|^2+|\mathbf{B}|^2}{2}$.

If $I \propto a^n$, with $n = +2$ or $n = -3$, the magnetic modes are generated during inflation with a scale invariant and frozen spectrum outside the horizon. Rather than assuming that I is an external function, one can obtain the required time dependence by assuming that I is a function of the inflaton ϕ, with a functional form related to the inflaton potential by [72, 73]

$$I = I_0 \exp\left[-\int \frac{n\, d\phi}{\sqrt{2\epsilon\,(\phi)} M_p}\right] \quad \Rightarrow \quad \langle I \rangle \propto a^n, \tag{2.9}$$

where ϵ is the usual slow-roll parameter, $\epsilon \equiv \frac{M_p^2}{2}\left(\frac{1}{V}\frac{dV}{d\phi}\right)^2$, with $M_p \equiv 1/\sqrt{8\pi G}$ denoting the reduced Planck mass.

Some recent work studied whether this coupling can result in visible cross-correlations between primordial perturbations and large-scale magnetic fields [58–60, 74–77]. This is not trivial to realize, as the $n = -3$ choice results in too large an energy density in the electric modes [42, 43], while $n = +2$ leads to too large an electromagnetic coupling constant during inflation [24, 43].[5]

For these reasons, we prefer not to identify the vector field as the electromagnetic field, and we discuss this model only as a mechanism for producing non-Gaussianity.[6] Indeed the vector modes are coupled to the inflaton field by the same $I^2\,(\phi)\,F^2$ term that generates them, and they source inflaton perturbations through this coupling. These perturbations add up incoherently to the inflaton vacuum modes, and are highly non-Gaussian.

Ref. [78] computed the resulting bispectrum, $\langle \zeta_{\mathbf{k}_1}\zeta_{\mathbf{k}_2}\zeta_{\mathbf{k}_3}\rangle$, in the equilateral configuration, i.e., $k_1 = k_2 = k_3$. The full bispectrum was computed in Refs. [24, 25]. The computations of Refs. [24, 25] are restricted to $n = 2$ and $n = -2$ which produce, respectively, scale invariant "magnetic" and "electric" perturbations. The model enjoys a symmetry $f \leftrightarrow \frac{1}{f}$, or $n \leftrightarrow -n$, under which $|E| \leftrightarrow |B|$. Both $\pm n$ result in the same equation for ζ. For brevity of exposition, we only refer to the $n = -2$ case in the reminder of this subsection. In this case one obtains, at the leading order in slow-roll,

$$E_k \simeq \frac{3H^2}{\sqrt{2}k^{3/2}} \quad , \quad B_k \simeq \frac{H}{\sqrt{2}k^{1/2}a} \quad , \quad k \ll aH \tag{2.10}$$

for the mode functions of each of the two polarizations of the "electric" and the "magnetic" fields in the super-horizon regime [25]. We note that the power in the "electric" field is frozen outside the horizon and scale invariant, whereas the power in the "magnetic" field decreases to negligible values.

Let us assume that, at the beginning of inflation, say at the time $t = 0$, the "electric" field has a classical homogeneous value, $\mathbf{E}^0$, all across the universe with negligible perturbations. For $n = -2$, the classical equations of motion for the vector field are solved by a constant, $\mathbf{E} = \mathbf{E}^0$. This quantity is, however, not the classical "electric" field that would be measured by a local observer at $t > 0$, which we denote by $\mathbf{E}_{\rm cl}$. In fact, the modes given by Eq. (2.10) become classical after they leave the horizon (we denote them as infra-red (IR) modes), and they add up with $\mathbf{E}^0$ to give $\mathbf{E}_{\rm cl}$. A given IR mode of wavelength λ averages to zero on

[5] These problems persist also for a general evolution of I beyond the a^n scaling [46].

[6] We continue to adopt the "electromagnetic" decomposition (2.8) for notational convenience.

regions of size $L \gg \lambda$, but it is constant in each region of the size $L \ll \lambda$, and it adds up stochastically with $\mathbf{E}^0$ and with all the other modes with $\lambda \gg L$ generated during inflation to determine the value $\mathbf{E}_{\rm cl}$ in that region. An observer at time $t > 0$ during inflation can only experience the value of $\mathbf{E}_{\rm cl}$ in its local Hubble patch. The average measured by this observer is drawn from a Gaussian distribution with the mean $\mathbf{E}^0$ and the variance given by

$$\langle \mathbf{E} \cdot \mathbf{E} \rangle = \frac{2 \times 4\pi}{(2\pi)^3} \int_{Ha(t=0)}^{Ha(t)} \frac{dk}{k} k^3 E_k^2 = \frac{9H^4}{2\pi^2} N, \tag{2.11}$$

where N is the number of e-folds from the start of inflation to the time t. The lower limit in the integral corresponds to the modes that left the horizon at the start of inflation (larger modes are not generated), while the upper limit corresponds to the modes that left the horizon at the time t (larger-momentum modes are still in the quantum regime and do not contribute to the classical average, $\mathbf{E}_{\rm cl}$, in the Hubble patch of length $\frac{1}{a(t)H}$).

The situation is completely identical to what happens to the so-called "stochastic inflation [79]," in which the variance of a massless scalar field, χ, is determined by the stochastic addition of the IR modes, and grows as $\langle \chi^2 \rangle \propto H^2 N$ during inflation. It is well established in that context that this variance contributes to the theoretical expectation value of the scalar field measure by local observers. This is customary used, for instance, in the Affleck-Dine model of baryogenesis [80] or in the curvaton field [81]. The fact that the vector field has spin 1 does not make any difference for these considerations, which simply follow from Eq. (2.10).

Let us consider a mode, ζ_k, of a given comoving momentum, k. This mode leaves the horizon N_k e-folds before the end of inflation. We are interested in the modes that affect the CMB anisotropies. Such modes leave the horizon $N_k \simeq N_{\rm CMB} \simeq 60$ e-folds before the end of inflation. The Hubble patch that they exit is the one that eventually becomes our Hubble patch. When the mode ζ_k leaves the horizon, the classical average of the "electric" field, $\mathbf{E}_{\rm cl}$, in this Hubble patch is drawn from a Gaussian distribution with the mean $\mathbf{E}^0$ and the variance given by Eq. (2.11), with $N = N_{\rm tot} - N_k$, where $N_{\rm tot}$ is the total number of e-folds of inflation.

In the presence of this mean, the kinetic term given in Eq. (2.7) results in the coupling of $\mathcal{L}_{\rm int} \simeq 4a^4 \mathbf{E}_{\rm cl} \cdot \delta\mathbf{E}\, \zeta$. This is the dominant operator for the part of ζ sourced by the vector field [25]. The power spectrum of ζ generated by this mechanism is given by

$$P_\zeta(k) = P_\zeta^{(0)}(k) \left[1 + g_*(k) \cos^2 \theta_{\hat{k},\hat{E}_{\rm cl}}\right] \quad , \quad g_*(k) \simeq -\frac{24 E_{\rm cl}^2 N_k^2}{\epsilon V(\phi)} \quad , \tag{2.12}$$

where $P_\zeta^{(0)} \equiv \frac{2\pi^2}{k^3} \frac{H^2}{8\pi^2 \epsilon M_p^2}$ is the square amplitude of the standard vacuum modes. The second term in Eq. (2.12) is the contribution of the sourced part of ζ, which (as phenomenologically required) we have assumed to be subdominant.[7] It follows from the N_k^2 proportionality that this term continues to grow in the super-horizon regime. This power spectrum was previously obtained in refs. [82–84] in the context of the anisotropic inflationary model [85], where however $E_{\rm cl}$ was identified with $\mathbf{E}^0$, missing the IR contribution.

[7] Non-detection of statistical anisotropy in the *WMAP* 9-year data after the correction of non-circular beam effects [13] would imply a conservative upper bound of $g_* \lesssim 0.1$.

The $\delta E\,\zeta$ mixing results in the following bispectrum in the squeezed limit, $k_3 \ll k_1 \approx k_2$ [25][8]

$$B_\zeta(k_1,k_2,k_3) \simeq 24 P_\zeta^{(0)}(k_1)\, P_\zeta^{(0)}(k_3)\, |g_*(k_1)|\, N_{k_3} \times \left[1 - \cos^2\theta_{\hat{k}_1,\,\hat{E}_{\rm cl}} - \cos^2\theta_{\hat{k}_3,\,\hat{E}_{\rm cl}} + \cos\theta_{\hat{k}_1,\,\hat{E}_{\rm cl}} \cos\theta_{\hat{k}_3,\,\hat{E}_{\rm cl}} \cos\theta_{\hat{k}_1,\,\hat{k}_3}\right]. \quad (2.13)$$

The predicted power spectrum (Eq. 2.12) and bispectrum (Eq. 2.13) break statistical isotropy, as $\mathbf{E}_{\rm cl}$ picks out a preferred direction. However, the prediction for an isotropic measurement is obtained by averaging Eq. (2.13) over all directions of $\hat{E}_{\rm cl}$. We find

$$B_\zeta(k_1,k_2,k_3)\Big|_{\text{isotropic measurement}} \simeq 8 P_\zeta^{(0)}(k_1)\, P_\zeta^{(0)}(k_3)\, |g_*(k_1)|\, N_{k_3}\left(1+\mu_{13}^2\right), \quad (2.14)$$

where $\mu_{13} \equiv \hat{\mathbf{k}}_1 \cdot \hat{\mathbf{k}}_3$. From this we obtain the Legendre coefficients in Eq. (1.1) as

$$c_0 = 32\,\frac{|g_*(k_1)|}{0.1}\,\frac{N_{k_3}}{60} \quad , \quad c_2 = \frac{c_0}{2}. \quad (2.15)$$

Due to simplicity of the model, Eq. (2.15) is a very predictive result, relating the bispectrum coefficients to the amount of statistical anisotropy of the power spectrum, i.e., g_*. This result holds for all models characterized by Eq. (2.7) and scale invariant "magnetic" or "electric" modes, including many analyses of the magnetogenesis mechanism [72] and of anisotropic inflation [85] (for which the departure from scale invariance is negligibly small; we note that in this work $\mathbf{E}^0$ evolves on an attractor solution, but this has no consequence for the accumulation of the IR modes). An analogous result will also hold for the model of Ref. [86] and for the mechanism of Ref. [87], for which the scalar perturbations have been studied in Ref. [88].

The smallness of g_* limits the level of non-Gaussianity. However, a larger bispectrum, for a given value of g_*, can be obtained if the model is more complicated. For instance, one can arrange for a triplet of U(1) vectors, and assume that they have classical vacuum expectation values which are orthogonal to one another and of equal magnitudes [89]. In this case the power spectrum is statistically isotropic ($g_* = 0$). This requires to assume that the IR sum is subdominant, as there is no reason to assume that the IR modes of the three vectors add up to orthonormal values. A larger bispectrum can also be obtained if there are additional fields and additional couplings, as in the waterfall mechanism of Ref. [90], in which a vector field of the kinetic term given in Eq. (2.7) is also coupled to the field that determines the end of hybrid inflation (see Ref. [25] for more detailed discussion).

2.3 Solid inflation

Ref. [26] studied a rather unusual model, in which inflation is driven by a system which has a field-theoretical description of a solid. An equivalent version of the model was proposed by Ref. [91], under the name of "elastic inflation."

Each volume element of the solid is characterized by a comoving label, ϕ^i (for instance, it can be the position of that element at the initial time $t = 0$). The functions, $\phi^i(t,\mathbf{x})$,

[8] See Ref. [25] for the full expression; due to different conventions, the bispectrum of Ref. [25] is the one given here divided by $(2\pi)^{3/2}$.

specify which volume element is located at a given position, $\mathbf{x}$, at a given time, t. A solid at rest in comoving coordinates then obeys

$$\langle \phi^1 \rangle = x \ , \ \langle \phi^2 \rangle = y \ , \ \langle \phi^3 \rangle = z \tag{2.16}$$

or, in short, $\langle \phi^i \rangle = x^i$. Even if the vacuum expectation value of each field is $\mathbf{x}$-dependent, a homogeneous and isotropic Friedmann-Robertson-Walker solution can still be obtained by requiring that the Lagrangian that controls the solid be invariant under rigid translations, $\phi^i \to \phi^i + a^i$, and SO(3) rotations, $\phi^i \to O^i_j \phi^j$.

At the lowest order in a derivative expansion, the translational invariance is guaranteed by considering functions

$$B^{ij} = g^{\mu\nu} \partial_\mu \phi^i \partial_\nu \phi^j, \tag{2.17}$$

and isotropy is obtained by requiring that the Lagrangian is a function of SO(3) invariants built from B^{ij}. Only three independent invariants exist, and Ref. [26] chose

$$S_{\rm solid} = \int d^4x \sqrt{-g} F\left[X, Y, Z\right] \ , \ X \equiv [B] \ , \ Y \equiv \frac{[B^2]}{[B]^2} \ , \ Z \equiv \frac{[B^3]}{[B]^3} \ , \tag{2.18}$$

where the square parenthesis denotes the trace of the corresponding matrix, e.g., $[B] \equiv \sum_i B^{ii}$.

The system has the energy-momentum tensor, $T^\mu_{\ \mu} = {\rm diag}\left(-\rho, p, p, p\right)$, with [26]

$$\rho = -F \ , \ p = F - \frac{2}{a^2} F_X \ , \tag{2.19}$$

where the subscript denotes a partial derivative, and F and F_X are evaluated on the background solutions given by $X = \frac{3}{a^2(t)}$, $Y = \frac{1}{3}$, and $Z = \frac{1}{9}$. These invariants are chosen in such a way that X is the only one affected by the overall physical volume expansion; this immediately explains as to why only the derivative of F with respect to X enters into the expression for the pressure.

Inflation is possible only if F is only mildly affected by the physical expansion, or, equivalently, only if F_X is sufficiently small. Specifically, we require

$$\epsilon \equiv -\frac{\dot{H}}{H} = \frac{X F_X}{F} \ll 1. \tag{2.20}$$

One also requires F_{XX} to be small, so that $\eta \equiv \frac{\dot{\epsilon}}{\epsilon H} \ll 1$ [26].

Let us now discuss cosmological perturbations in this system. It is convenient to work in a spatially flat gauge, where the dynamical scalar and vector perturbations are all encoded in the perturbations of the scalar fields:

$$\delta\phi^i = \pi^i\left(t, \mathbf{x}\right) = \frac{\partial_i}{\sqrt{-\nabla^2}} \pi_L + \pi^i_T \ , \tag{2.21}$$

where the vector components are transverse, $\partial_i \pi^i_T = 0$. The scalar and vector modes are decoupled from each other at the linearized level.[9] At the lowest order in the slow roll

[9] As always in cosmology, the sectors of scalar and vector perturbations also include non-dynamical modes which are, in the spatially flat gauge, encoded in the $\delta g_{0\mu}$ metric components. These fields can be integrated out as explained in [26]. This affects the action for the dynamical modes, π_L and π^i_T, at long wavelengths. Finally, there are also tensor perturbations - the gravity waves - encoded in the δg_{ij} metric components, and which we do not discuss here.

parameters, and in the deep sub-horizon regime, the sound speeds of the scalar (longitudinal) modes, c_L, and vector (transverse) modes, c_T, are given, respectively, by [26]

$$c_L^2 \simeq \frac{1}{3} + \frac{8}{9}\frac{F_Y + F_Z}{X F_X} \ , \quad c_T^2 \simeq \frac{3}{4}\left(1 + c_L^2\right) \ , \tag{2.22}$$

so that the propagation is subluminal and non-tachyonic ($0 < c_L^2 < 1$ and $0 < c_T^2 < 1$) for $0 < F_Y + F_Z < \frac{3}{8}\epsilon|F|$ [26]. Namely, the requirement of an accelerated expansion forces F_X to be small, while subluminality also requires that the combination $F_Y + F_Z$ be small. Finally, the theory involves derivative interactions of the "phonon" fields, π^i, which necessarily become strong at some scale Λ. A detailed study in Ref. [26] gives an estimate of $\Lambda \gg H$ (so that the linearized theory is also valid in the sub-horizon regime, up to Λ), provided that $\epsilon c_L^3 \gg \left(\frac{H}{M_p}\right)^{2/3}$, which can always be obtained for a sufficiently small H.

In a conformally flat gauge, the gauge-invariant scalar perturbation, ζ, evaluates to $\zeta = -H\frac{\delta\rho}{\dot\rho} = \frac{1}{3}\partial\pi$. Its solution exhibits two features that are peculiar in scalar-field inflation models, but that were nevertheless already seen in the models studied in the previous subsection [24]. The first one is the fact that ζ is not conserved on super-horizon scales, due to the anisotropic stress that does not vanish on super-horizon scales [26]. Indeed, following Ref. [26], we obtain

$$\delta T_{ij,\mathrm{scalar}} = a^2 M_p^2 \dot H \zeta \left[2\left(3 - 2\epsilon + \eta\right)\delta_{ij} - \left(3 + 3c_L^2 - 2\epsilon + \eta\right)\left(3\hat k_i\,\hat k_j - \delta_{ij}\right)\right] . \tag{2.23}$$

Let us recall that, also for the model described by Eq. (2.7), the anisotropic component of the stress-energy tensor, $\propto E_{\mathrm{cl},i}\delta E_j$, does not vanish outside the horizon, and thus the anisotropic term in Eq. (2.12) grows outside the horizon.

The second feature is that, analogously to the model described by Eq. (2.7), the bispectrum of solid inflation is largest in the squeezed configurations, and exhibits a nontrivial dependence on the angle between the modes in the squeezed limit. The dominant contribution to the bispectrum is given by the interactions of π encoded in the scalar field Lagrangian, while the metric perturbations provide a negligible contribution. The dominant interaction in a slow roll expansion is given by [26]

$$\mathcal{L} \supset M_p^2 a^3 H^2 \frac{F_Y}{F}\left[\frac{7}{81}\left(\partial\pi\right)^2 - \frac{1}{9}\partial\pi\partial_j\pi^k\partial_k\pi^j - \frac{4}{9}\partial\pi\partial_j\pi^k\partial_j\pi^k + \frac{2}{3}\partial_j\pi^i\partial_j\pi^k\partial_k\pi^i\right] . \tag{2.24}$$

Also in this respect, the situation is analogous to the model discussed in the previous subsection, where the dominant contribution to the bispectrum is obtained from Eq. (2.7), disregarding metric perturbations. When written in terms of ζ, this interaction exhibits nontrivial dependence on the direction of the modes which does not vanish in the squeezed limit, imprinting the nontrivial angular dependence in the bispectrum.

At the leading order, the Legendre coefficients in Eq. (1.1) are given by [26]

$$c_0 \simeq 0 \ , \quad c_2 = \mathcal{O}\left(1\right)\frac{F_Y}{F}\frac{1}{\epsilon c_L^2} . \tag{2.25}$$

Namely, in the squeezed limit, the dominant contribution is given by the quadrupole term, whereas the monopole term is negligible. The dominant quadrupole term is essentially proportional to a free combination of parameters (we recall that avoiding superluminality and strong coupling at $p \lesssim H$ imposes restrictions on the combination $F_Y + F_Z$ but not on F_Y or F_Z individually).

3 Signatures in the cosmic microwave background

In this section, we shall derive the flat-sky (Sec 3.1) and full-sky (Sec 3.2) formulae for the bispectrum of CMB temperature anisotropy from the bispectrum of curvature perturbations given in Eq. (1.1). We then calculate, in Sec. 3.3, the error bars of c_0, c_1, and c_2 expected for a cosmic-variance-limited experiment measuring temperature anisotropy up to $\ell = 2000$.

3.1 Flat-sky formula

While the full-sky formula is eventually needed for the analysis of full-sky temperature maps, let us derive first the flat-sky formula, as the flat-sky formula is usually simpler and more intuitively understandable.

Under the flat-sky approximation, which is valid only on sufficiently small angular scales, $\ell \gg 1$, CMB fluctuations on the sky are expanded using the two-dimensional Fourier transform, instead of the spherical harmonics. The Fourier coefficients of CMB anisotropy, $a(\boldsymbol{\ell})$ are related to the three-dimensional coefficients of the curvature perturbation, $\zeta(\mathbf{k})$, as [92]

$$a(\boldsymbol{\ell}) = \int_0^{\tau_0} d\tau \int_{-\infty}^{\infty} \frac{dk_z}{2\pi} \zeta\left(\mathbf{k}^{\parallel} = -\frac{\boldsymbol{\ell}}{D}, k_z\right) S_I\left(k = \sqrt{k_z^2 + (\ell/D)^2}, \tau\right) \frac{1}{D^2} e^{-ik_z D} \ , \quad (3.1)$$

where $\mathbf{k}^{\parallel} \equiv (k_x, k_y)$, $D \equiv \tau_0 - \tau$ is the conformal distance out to a given epoch τ, τ_0 is the present-day conformal time, and S_I is the so-called source function.[10] This relation simply tells us that $a(\boldsymbol{\ell})$ measures the ζ modes that are perpendicular to the line-of-sight direction (i.e., the modes on the sky), and the line-of-sight modes are washed out by integration.

It is straightforward to compute the bispectrum of $a(\boldsymbol{\ell})$ following, e.g., Ref. [92]:

$$\langle a(\boldsymbol{\ell}_1) a(\boldsymbol{\ell}_2) a(\boldsymbol{\ell}_3) \rangle = (2\pi)^2 \delta^{(2)}\left(\boldsymbol{\ell}_1 + \boldsymbol{\ell}_2 + \boldsymbol{\ell}_3\right) \sum_L c_L b^L(\ell_1, \ell_2, \ell_3) \ , \quad (3.2)$$

where

$$b^L(\ell_1, \ell_2, \ell_3) \equiv \int_{-\infty}^{\infty} r^2 dr \left[\prod_{n=1}^{3} \int_0^{\tau_0} d\tau_n \int_{\ell_n/D_n}^{\infty} \frac{dk_n}{2\pi} \mathcal{G}(\ell_n, k_n, \tau_n, r)\right] \times \left[\sum_{n=0}^{L} (\hat{\boldsymbol{\ell}}_1 \cdot \hat{\boldsymbol{\ell}}_2)^n \mathcal{F}_L^{(n)}\right] P_\zeta(k_1) P_\zeta(k_2) + (2 \text{ perm}) \ , \quad (3.3)$$

with

$$\mathcal{G}(\ell, k, \tau, r) \equiv \left[1 - \left(\frac{\ell}{kD}\right)^2\right]^{-1/2} S_I(k, \tau) \frac{2}{D^2} \cos\left[\sqrt{1 - \left(\frac{\ell}{kD}\right)^2} k(r - D)\right] \ . \quad (3.4)$$

[10] The source function is related to the radiation transfer function defined in Eq. (3.9) as $\mathcal{T}_\ell(k) = \int_0^{\tau_0} d\tau \ S_I(k, \tau) j_\ell(kD)$.

The other kernel functions, $\mathcal{F}_L^{(n)}$, for $L \leq 2$ are given by $\mathcal{F}_0^{(0)} = 1$, $\mathcal{F}_1^{(1)} = \prod_{n=1}^2 \frac{\ell_n}{k_n D_n}$, $\mathcal{F}_2^{(2)} = \frac{3}{2}\prod_{n=1}^2 \left(\frac{\ell_n}{k_n D_n}\right)^2$, and

$$\mathcal{F}_1^{(0)} = -\prod_{n=1}^{2}\sqrt{1-\left(\frac{\ell_n}{k_n D_n}\right)^2}\tan\left[\sqrt{1-\left(\frac{\ell_n}{k_n D_n}\right)^2}k_n(r-D_n)\right], \tag{3.5}$$

$$\mathcal{F}_2^{(0)} = \frac{3}{2}\prod_{n=1}^{2}\left[1-\left(\frac{\ell_n}{k_n D_n}\right)^2\right] - \frac{1}{2}, \tag{3.6}$$

$$\mathcal{F}_2^{(1)} = -3\prod_{n=1}^{2}\frac{\ell_n}{k_n D_n}\sqrt{1-\left(\frac{\ell_n}{k_n D_n}\right)^2}\tan\left[\sqrt{1-\left(\frac{\ell_n}{k_n D_n}\right)^2}k_n(r-D_n)\right]. \tag{3.7}$$

While these formulae are still complicated, one can read off the leading behaviours of these expressions in the small-scale limit, in which the dominant contributions in the k integration come from the modes with $k \approx \ell/D$. In this limit the kernel functions become $\mathcal{F}_1^{(0)} \to 0$, $\mathcal{F}_2^{(1)} \to 0$, $\mathcal{F}_1^{(1)} \to 1$, $\mathcal{F}_2^{(0)} \to -1/2$, and $\mathcal{F}_2^{(2)} \to 3/2$. We thus find

$$\begin{aligned} b^L(\ell_1,\ell_2,\ell_3) \to \int_{-\infty}^{\infty} r^2 dr \left[\prod_{n=1}^{3}\int_0^{\tau_0} d\tau_n \int_{\ell_n/D_n}^{\infty}\frac{dk_n}{2\pi}\mathcal{G}(\ell_n,k_n,\tau_n,r)\right] \\ \times P_L(\hat{\boldsymbol{\ell}}_1\cdot\hat{\boldsymbol{\ell}}_2)P_\zeta(k_1)P_\zeta(k_2) + (2\text{ perm}). \end{aligned} \tag{3.8}$$

This result shows that the CMB bispectrum is proportional to $P_L(\hat{\boldsymbol{\ell}}_1\cdot\hat{\boldsymbol{\ell}}_2)$ (and its permutations), which is expected from $P_L(\hat{\mathbf{k}}_1\cdot\hat{\mathbf{k}}_2)$ (and its permutations) in the three-dimensional bispectrum of the primordial curvature perturbation.

While the approximation of $\ell \approx kD$ gives a simple and transparent result given in Eq. (3.8), it is less precise than the original form given by Eq. (3.3). In Appendix A, we discuss the precision of Eqs. (3.3) and (3.8) with respect to the full-sky result given in the next subsection.

3.2 Full-sky formula

Encouraged by the flat-sky results, we now move onto the full-sky case. The CMB temperature anisotropy on the celestial sphere is expanded by the spherical harmonic function as $\delta T(\hat{\mathbf{n}})/T = \sum_{\ell,m} a_{\ell m} Y_{\ell m}(\hat{\mathbf{n}})$, where $\hat{\mathbf{n}}$ is a three-dimensional unit vector pointing toward a given direction on the sky. The spherical harmonics coefficients, $a_{\ell m}$, are related to the primordial curvature perturbation as

$$\begin{aligned} a_{\ell m} &= 4\pi(-i)^\ell \int \frac{d^3\mathbf{k}}{(2\pi)^3}\mathcal{T}_\ell(k)\zeta_{\mathbf{k}}Y^*_{\ell m}(\hat{\mathbf{k}}) \\ &= 4\pi(-i)^\ell \int \frac{k^2 dk}{(2\pi)^3}\mathcal{T}_\ell(k)\zeta_{\ell m}(k), \end{aligned} \tag{3.9}$$

where $\mathcal{T}_\ell(k)$ is the so-called radiation transfer function, and we have defined the curvature perturbation expanded in spherical harmonics as $\zeta_{\ell m}(k) \equiv \int d^2\hat{\mathbf{k}}\ \zeta_{\mathbf{k}}Y^*_{\ell m}(\hat{\mathbf{k}})$. Then, the bispectrum of $a_{\ell m}$ can be straightforwardly calculated as

$$\left\langle\prod_{n=1}^{3}a_{\ell_n m_n}\right\rangle = \left[\prod_{n=1}^{3}4\pi(-i)^{\ell_n}\int\frac{k_n^2 dk_n}{(2\pi)^3}\mathcal{T}_{\ell_n}(k_n)\right]\left\langle\prod_{n=1}^{3}\zeta_{\ell_n m_n}(k_n)\right\rangle, \tag{3.10}$$

with the bispectrum of $\zeta_{\ell m}$ related to $B_\zeta(k_1, k_2, k_3)$ as

$$\left\langle \prod_{n=1}^{3} \zeta_{\ell_n m_n}(k_n) \right\rangle = \left[\prod_{n=1}^{3} \int d^2\hat{\mathbf{k}}_n Y^*_{\ell_n m_n}(\hat{\mathbf{k}}_n) \right] (2\pi)^3 \delta^{(3)}\left(\mathbf{k}_1 + \mathbf{k}_2 + \mathbf{k}_3\right) B_\zeta(k_1, k_2, k_3). \tag{3.11}$$

Using the bispectrum of ζ given in Eq. (1.1), $B_\zeta(k_1, k_2, k_3)$ can be expanded as

$$B_\zeta(k_1, k_2, k_3) = P_\zeta(k_1) P_\zeta(k_2) \sum_L c_L \frac{4\pi}{2L+1} \sum_M Y^*_{LM}(\hat{\mathbf{k}}_1) Y_{LM}(\hat{\mathbf{k}}_2) + (2 \text{ perm}). \tag{3.12}$$

Using the definition of the delta function, $\delta^{(3)}(\mathbf{k}) = (2\pi)^{-3} \int d^3\mathbf{x}\, e^{i\mathbf{k}\cdot\mathbf{x}}$, we also expand the delta function as

$$\begin{aligned} \delta^{(3)}\left(\mathbf{k}_1 + \mathbf{k}_2 + \mathbf{k}_3\right) = 8 \int_0^\infty r^2 dr \left[\prod_{n=1}^{3} \sum_{L_n M_n} (-1)^{\frac{L_n}{2}} j_{L_n}(k_n r) Y^*_{L_n M_n}(\hat{\mathbf{k}}_n) \right] \\ \times \begin{pmatrix} L_1 & L_2 & L_3 \\ M_1 & M_2 & M_3 \end{pmatrix} I_{L_1 L_2 L_3} \ , \end{aligned} \tag{3.13}$$

where the 2×3 matrix denotes the Wigner-3j symbol, and the I symbol is defined by

$$I_{l_1 l_2 l_3} \equiv \sqrt{\frac{(2l_1+1)(2l_2+1)(2l_3+1)}{4\pi}} \begin{pmatrix} l_1 & l_2 & l_3 \\ 0 & 0 & 0 \end{pmatrix} . \tag{3.14}$$

Now, performing the integrals of the spherical harmonics over $\hat{\mathbf{k}}_1, \hat{\mathbf{k}}_2$, and $\hat{\mathbf{k}}_3$, and performing the summations over M_1, M_2, M_3, and M as described in Ref. [93], we obtain

$$\left\langle \prod_{n=1}^{3} \zeta_{\ell_n m_n}(k_n) \right\rangle = (2\pi)^3 B_{\zeta, \ell_1 \ell_2 \ell_3}(k_1, k_2, k_3) \begin{pmatrix} \ell_1 & \ell_2 & \ell_3 \\ m_1 & m_2 & m_3 \end{pmatrix} , \tag{3.15}$$

where

$$\begin{aligned} B_{\zeta, \ell_1 \ell_2 \ell_3}(k_1, k_2, k_3) = 8 \int_0^\infty r^2 dr \left[\prod_{n=1}^{3} \sum_{L_n} (-1)^{\frac{L_n}{2}} j_{L_n}(k_n r) \right] I_{L_1 L_2 L_3} \\ \times \sum_L c_L \frac{4\pi}{2L+1} I_{\ell_1 L_1 L} I_{\ell_2 L_2 L} (-1)^{\ell_2 + L_1} \delta_{L_3, \ell_3} \\ \times \begin{Bmatrix} \ell_1 & \ell_2 & \ell_3 \\ L_2 & L_1 & L \end{Bmatrix} P_\zeta(k_1) P_\zeta(k_2) + (2 \text{ perm}) \ . \end{aligned} \tag{3.16}$$

Here, the 2×3 matrix enclosed by curly brackets denotes the Wigner-6j symbol. As the primordial bispectrum given by Eq. (1.1) is rotationally invariant, the bispectrum expanded in spherical harmonics must also be rotationally invariant. This means that the dependence of the bispectrum on m_1, m_2 and m_3 must be given by the Wigner-3j symbol, as shown in Eq. (3.15). This property ensures rotational invariance of the CMB bispectrum.

Substituting Eqs. (3.15) and (3.16) into Eq. (3.10), we finally obtain the full-sky formula for the CMB bispectrum:

$$\left\langle \prod_{n=1}^{3} a_{\ell_n m_n} \right\rangle = \begin{pmatrix} \ell_1 & \ell_2 & \ell_3 \\ m_1 & m_2 & m_3 \end{pmatrix} B_{\ell_1 \ell_2 \ell_3} = \begin{pmatrix} \ell_1 & \ell_2 & \ell_3 \\ m_1 & m_2 & m_3 \end{pmatrix} \sum_L c_L B^L_{\ell_1 \ell_2 \ell_3} \ , \tag{3.17}$$

where

$$B^L_{\ell_1\ell_2\ell_3} \equiv \int_0^\infty r^2 dr \left[\prod_{n=1}^{3}\sum_{L_n}(-1)^{\frac{\ell_n+L_n}{2}}\right] I_{L_1L_2L_3}\beta_{\ell_1L_1}(r)\beta_{\ell_2L_2}(r)\alpha_{\ell_3}(r)$$
$$\times\frac{4\pi}{2L+1}I_{\ell_1L_1L}I_{\ell_2L_2L}(-1)^{\ell_2+L_1}\delta_{L_3,\ell_3}\left\{\begin{array}{ccc}\ell_1 & \ell_2 & \ell_3\\ L_2 & L_1 & L\end{array}\right\} + (2\text{ perm})\ , \qquad (3.18)$$

and

$$\alpha_\ell(r) \equiv \frac{2}{\pi}\int_0^\infty k^2 dk\ \mathcal{T}_\ell(k) j_\ell(kr)\ , \qquad (3.19)$$

$$\beta_{\ell L}(r) \equiv \frac{2}{\pi}\int_0^\infty k^2 dk\ P_\zeta(k)\mathcal{T}_\ell(k) j_L(kr)\ . \qquad (3.20)$$

Owing to the selection rules of the Wigner symbols, ℓ_1, ℓ_2 and ℓ_3 are constrained by parity invariance and the triangular condition:

$$\ell_1+\ell_2+\ell_3 = \text{even}\ , \quad |\ell_1-\ell_2| \le \ell_3 \le \ell_1+\ell_2\ . \qquad (3.21)$$

The former constraint is a consequence of the bispectrum of curvature perturbations given by Eq. (1.1) being parity-even. The summation ranges of L_1 and L_2 are also restricted to

$$L_n = |\ell_n - L|, |\ell_n - L|+2, \cdots, \ell_n+L-2, \ell_n+L\ . \qquad (3.22)$$

In the full-sky formula given by Eq. (3.18), the angle dependence for $L > 0$ induces a coupling among ℓ_1, ℓ_2 and ℓ_3 via the Wigner-6j symbol. As a result, Eq. (3.18) is not separable (or at least not obviously separable) with respect to ℓ's unlike the usual local-form CMB bispectrum without angle dependence, i.e., $L = 0$.

Figures 2 and 3 show the absolute values of the full-sky reduced bispectra, $b^L_{\ell_1\ell_2\ell_3} \equiv B^L_{\ell_1\ell_2\ell_3}\left(I_{\ell_1\ell_2\ell_3}\right)^{-1}$, for $L = 0$, 1, and 2. Note that the full-sky reduced bispectrum reduces to the flat-sky bispectrum, $b(\ell_1, \ell_2, \ell_3)$, that we discussed in the previous subsection, in the small-sky limit [7].

Figure 2 shows the equilateral triangles with $\ell \equiv \ell_1 = \ell_2 = \ell_3$, while Figure 3 shows triangles with $\ell_1 = \ell_2 = 200$, which become squeezed triangles for $\ell_3 \ll 200$. We find that the amplitudes of the equilateral triangles monotonically decrease as L increases. We can understand this by using the flat-sky formula given in Eq. (3.8): the Legendre polynomials give the ratio of $L = 0$, 1, and 2 terms as

$$b^{L=0}(\ell,\ell,\ell) : b^{L=1}(\ell,\ell,\ell) : b^{L=2}(\ell,\ell,\ell) = 1 : -\frac{1}{2} : -\frac{1}{8}, \qquad (3.23)$$

for $\hat{\boldsymbol{\ell}}_i \cdot \hat{\boldsymbol{\ell}}_j = -\frac{1}{2}$ $(i \neq j)$.

Figure 3 shows the squeezed triangles with $\ell_3 \ll \ell_1 = \ell_2 = 200$. In the squeezed limit, the CMB bispectrum of $L = 1$ is highly suppressed compared with those of $L = 0$ and 2. This is simply due to symmetry: the $L = 1$ term vanishes in the exact squeezed limit. Again, the flat-sky formula given in Eq. (3.8) gives the ratio of $L = 0$, 1, and 2 terms as

$$b^{L=0}(\ell_1,\ell_1,\ell_3) : b^{L=1}(\ell_1,\ell_1,\ell_3) : b^{L=2}(\ell_1,\ell_1,\ell_3) = 1 : 0 : -\frac{1}{2}, \qquad (3.24)$$

for $\hat{\boldsymbol{\ell}}_1 \cdot \hat{\boldsymbol{\ell}}_3 = 0 = \hat{\boldsymbol{\ell}}_2 \cdot \hat{\boldsymbol{\ell}}_3$.

As these calculations are quite involved, we provide the simplified analytical formula in the Sachs–Wolfe limit in Appendix B. This test validates our numerical results shown in Figures 2 and 3.

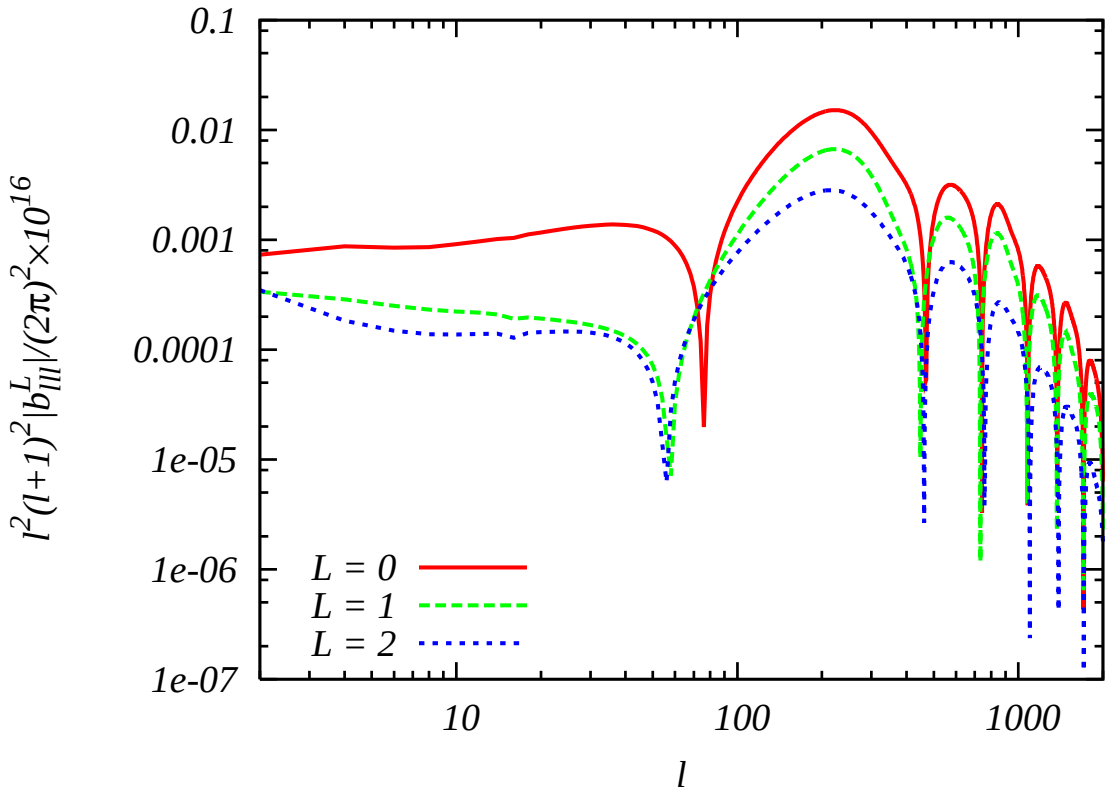

Figure 2. Absolute values of the *equilateral* CMB temperature reduced bispectra, $|b^L_{\ell\ell\ell}|$, for $L = 0$ (solid), $L = 1$ (long-dashed), and $L = 2$ (short-dashed).

3.3 Expected uncertainties on c_1 and c_2

In this subsection, we calculate the 1-σ error bars of c_0, c_1 and c_2, i.e., δc_0, δc_1, and δc_2, expected for a cosmic-variance-limited experiment measuring temperature anisotropy. Here, we shall focus on a simultaneous estimation of a pair of parameters: (c_0, c_1) and (c_0, c_2). We give the full constraint varying all three parameters simultaneously in Appendix C.

Following Ref. [7], we calculate the Fisher matrix, $F_{LL'}$, from

$$F_{LL'} \equiv \sum_{2\le\ell_1\le\ell_2\le\ell_3\le\ell_{\rm max}} \frac{B^L_{\ell_1\ell_2\ell_3} B^{L'}_{\ell_1\ell_2\ell_3}}{\sigma^2_{\ell_1\ell_2\ell_3}} \ , \tag{3.25}$$

where the variance of the CMB bispectrum, $\sigma^2_{\ell_1\ell_2\ell_3}$, is given by

$$\sigma^2_{\ell_1\ell_2\ell_3} = C_{\ell_1} C_{\ell_2} C_{\ell_3} \left[(-1)^{\ell_1+\ell_2+\ell_3} (1 + 2\delta_{\ell_1,\ell_2}\delta_{\ell_2,\ell_3}) + \delta_{\ell_1,\ell_2} + \delta_{\ell_2,\ell_3} + \delta_{\ell_3,\ell_1} \right] \ , \tag{3.26}$$

with C_ℓ being the power spectrum of temperature fluctuations. As we consider a cosmic-variance-limited experiment, we ignore instrumental noise here.

As we show in Appendix C, c_0 and c_1 are nearly uncorrelated, so are c_0 and c_2; however, c_1 and c_2 are highly correlated. Therefore, in this subsection, we shall consider submatrices of $F_{LL'}$ involving only either (c_0, c_1) or (c_0, c_2), and study the full matrix in Appendix C.

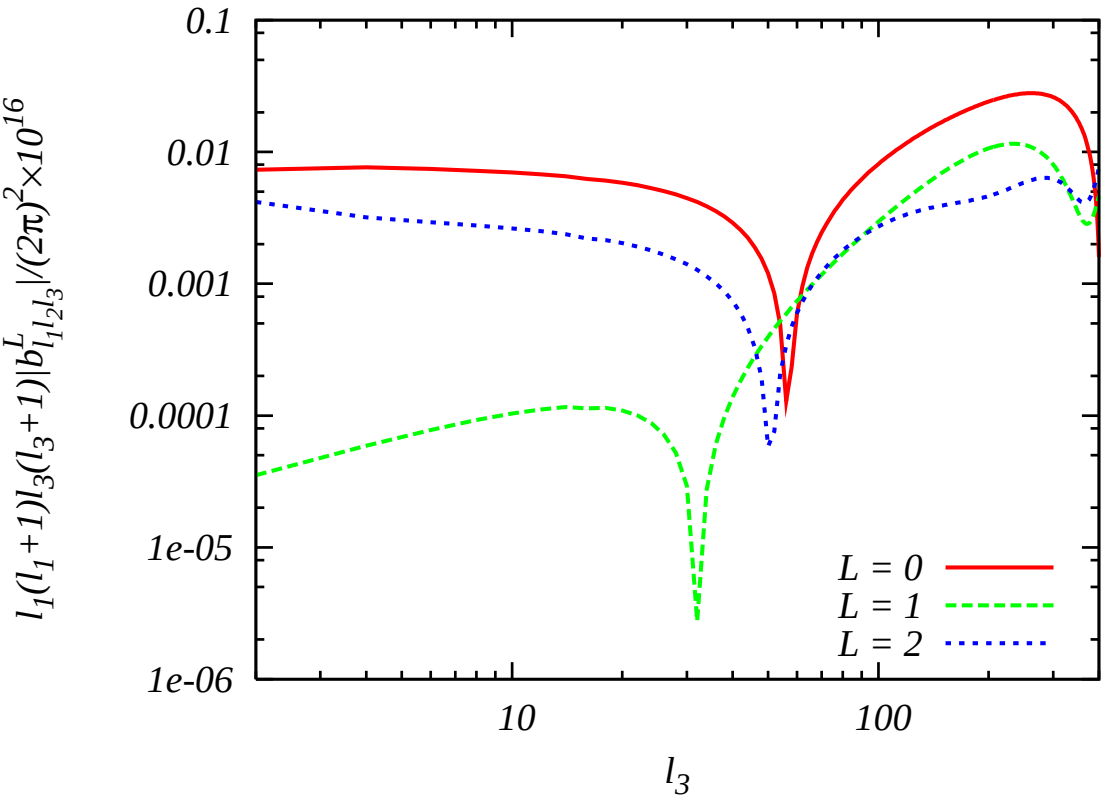

Figure 3. Same as Figure 3, but for the *squeezed* triangles, $|b^L_{\ell_1\ell_2\ell_3}|$, with $\ell_1 = \ell_2 = 200$, as a function of ℓ_3.

We define the submatrix (a 2×2 matrix) as

$$ {}^{(2)}F_{ij} \equiv \begin{pmatrix} F_{00} & F_{0L} \\ F_{L0} & F_{LL} \end{pmatrix} , \tag{3.27} $$

where L takes on either 1 or 2. The 1-σ marginalized error bars are then given by the matrix inverse as $(\delta c_0, \delta c_L) = \left(\sqrt{{}^{(2)}F^{-1}_{11}}, \sqrt{{}^{(2)}F^{-1}_{22}}\right)$.

In Figure 4, we show the ratios of error bars, $\delta c_1/\delta c_0$ and $\delta c_2/\delta c_0$, as a function of the maximum multipole in the sum, $\ell_{\rm max}$. The solid and short-dashed lines show the exact results for $L = 1$ and $L = 2$, respectively, while the long-dashed and dotted lines show the corresponding Sachs–Wolfe approximations for $L = 1$ and $L = 2$, respectively. We find that the Sachs–Wolfe approximations trace the overall behavior of the exact calculations well.

The error bar on c_1 is an order of magnitude larger than that on c_0 for $\ell_{\rm max} \gtrsim 100$, as the $L = 1$ bispectrum has a vanishing amplitude in the squeezed limit. On the other hand, the error bar on c_2 is comparable to that on c_0: the Sachs–Wolfe approximation gives an asymptotic relation of $\delta c_2 = 4\delta c_0$. The exact calculation gives $\delta c_2 \approx 3\delta c_0$ for $\ell_{\rm max} = 2000$.

Finally, the 1-σ error bars expected for a cosmic-variance-limited experiment measuring

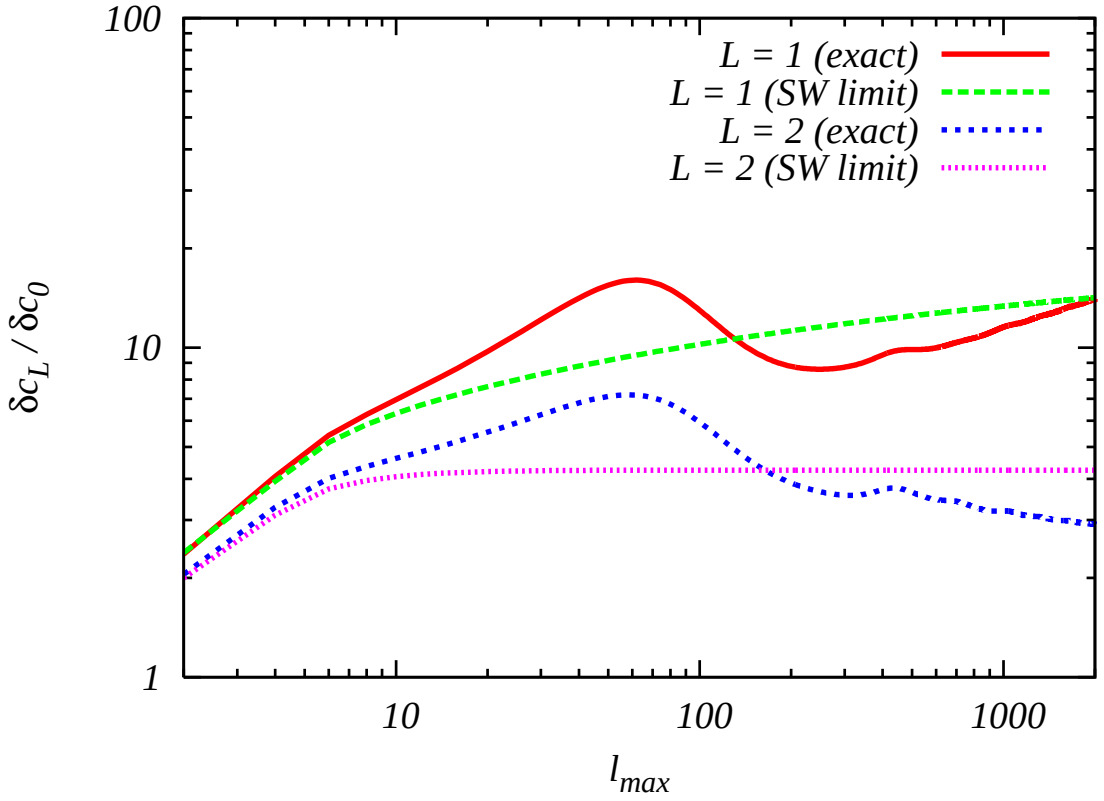

Figure 4. Ratios of the expected error bars, $\delta c_L/\delta c_0$ ($L = 1$ and 2), as a function of the maximum multipoles in the sum, $\ell_{\rm max}$. The solid and short-dashed lines show the exact results for $L = 1$ and $L = 2$, respectively, while the long-dashed and dotted lines show the corresponding Sachs–Wolfe approximations for $L = 1$ and $L = 2$, respectively. We find that the Sachs–Wolfe approximations trace the overall behavior of the exact calculations well.

temperature anisotropy up to $\ell_{\rm max} = 2000$ are given by

$$(\delta c_0, \delta c_1) = (4.4, 61) \ , \tag{3.28}$$

$$(\delta c_0, \delta c_2) = (4.4, 13) \ . \tag{3.29}$$

See Eq. (C.1) for the full Fisher matrix.

4 Consistency relations with higher spin fields

Primordial correlation functions in the limit that some combinations of external momenta go to zero – *soft limits* – play a special role in constraining the physics of inflation. Significant squeezed non-Gaussianity is associated with the presence of extra light degrees of freedom during inflation, hence soft limits can be understood as probing the spectrum of light fields in the early universe. Moreover, soft limits are observationally relevant and are subject to a number of interesting theoretical consistency relations. The first example of such a consistency relation was noted in [12] and established under much more general conditions in [1]: $\lim_{k_3\to 0} B_\zeta(k_1, k_2, k_3) = (1 - n_s)P_\zeta(k_1)P_\zeta(k_3)$. This holds independently of the inflationary

Lagrangian, under the assumption that there is only a single field, an attractor solution has been reached [5, 6], and the initial state is in a Bunch-Davies state [3, 4].

Our new parametrization given by Eq. (1.1) represents a non-trivial modification of this consistency relation:

$$\lim_{k_3\to 0} B_\zeta(k_1,k_2,k_3) = \left(2\sum_L c_L P_L(\hat{\mathbf{k}}_1\cdot\hat{\mathbf{k}}_3)\right) P_\zeta(k_1)P_\zeta(k_3)\,. \tag{4.1}$$

The possibility that some of the c_L coefficients can be $\gg |n_s-1| \sim 10^{-2}$ indicates extra light fields in the early universe, while the non-trivial angular dependence is associated with anisotropic sources (such as higher spin fields). We also expect non-trivial soft limits for higher-order correlation functions. To explore such effects, we introduce the quantities

$$f_{NL}^{\rm eff}(k_i) \equiv \lim_{k_3\to 0} \frac{5}{12}\frac{B_\zeta(k_1,k_2,k_3)}{P_\zeta(k_1)P_\zeta(k_3)}\,, \tag{4.2}$$

$$\tau_{NL}^{\rm eff}(k_i) \equiv \lim_{\mathbf{k_1}+\mathbf{k_2}\to 0} \frac{1}{4}\frac{T_\zeta(k_1,k_2,k_3,k_4)}{P_\zeta(|\mathbf{k}_1+\mathbf{k}_2|)P_\zeta(k_1)P_\zeta(k_3)}\,, \tag{4.3}$$

where $\langle\zeta_{\mathbf{k}_1}\zeta_{\mathbf{k}_2}\zeta_{\mathbf{k}_3}\zeta_{\mathbf{k}_4}\rangle = (2\pi)^3\delta^{(3)}(\sum_i \mathbf{k}_i)T_\zeta(k_1,k_2,k_3,k_4)$. For the local-type non-Gaussianity the quantities $f_{NL}^{\rm eff}$ and $\tau_{NL}^{\rm eff}$ become the standard (momentum independent) non-linearity parameters. In this case there is an interesting consistency relation:

$$\tau_{NL} \geq \left(\frac{6}{5}f_{NL}\right)^2\,, \tag{4.4}$$

where we dropped the superscript "eff" to emphasize that this relation is understood in the case where Eqs. (4.2) and (4.3) are independent of momenta. This relation was first noted by Suyama and Yamaguchi in [16] and further explored in [17–21].

In this subsection, we explore the non-Gaussianity consistency relations in the context of the $I^2(\phi)F^2$ model given in Eq. (2.7). In general this model breaks statistical isotropy, as discussed in Sec. 2.2. From Eq. (2.13) we obtain

$$f_{NL}^{\rm eff} \simeq 10N_{k_1}^2 N_{k_3}\frac{24E_{\rm cl}^2}{\epsilon V(\phi)}\left[1-\cos^2\theta_{\hat{k}_1,\hat{E}_{\rm cl}}-\cos^2\theta_{\hat{k}_3,\hat{E}_{\rm cl}}+\cos\theta_{\hat{k}_1,\hat{E}_{\rm cl}}\cos\theta_{\hat{k}_3,\hat{E}_{\rm cl}}\cos\theta_{\hat{k}_1,\hat{k}_3}\right]\,, \tag{4.5}$$

where we recall that $|g_*(N_{k_i})| = N_{k_i}^2\frac{24E_{\rm cl}^2}{\epsilon V(\phi)} \ll 1$ is assumed.

We compute the trispectrum for the first time in the model given by Eq. (2.7). The computation follows very closely the analogous one of the bispectrum performed in [25], and so we omit the technical details. We obtain

$$\begin{aligned}\tau_{\rm NL}^{\rm eff} \simeq 144N_{k_1}^2N_{k_3}^2\frac{24E_{\rm cl}^2}{\epsilon V(\phi)}\Big[&1-\cos^2\theta_{\hat{k}_1,\hat{E}_{\rm cl}}-\cos^2\theta_{\hat{k}_{12},\hat{E}_{\rm cl}}-\cos^2\theta_{\hat{k}_3,\hat{E}_{\rm cl}}\\
&+\cos\theta_{\hat{k}_1,\hat{E}_{\rm cl}}\cos\theta_{\hat{k}_3,\hat{E}_{\rm cl}}\cos\theta_{\hat{k}_1,\hat{k}_3}\\
&+\cos\theta_{\hat{k}_1,\hat{E}_{\rm cl}}\cos\theta_{\hat{k}_{12},\hat{E}_{\rm cl}}\cos\theta_{\hat{k}_1,\hat{k}_{12}}\\
&+\cos\theta_{\hat{k}_{12},\hat{E}_{\rm cl}}\cos\theta_{\hat{k}_3,\hat{E}_{\rm cl}}\cos\theta_{\hat{k}_{12},\hat{k}_3}\\
&-\cos\theta_{\hat{k}_1,\hat{E}_{\rm cl}}\cos\theta_{\hat{k}_3,\hat{E}_{\rm cl}}\cos\theta_{\hat{k}_1,\hat{k}_{12}}\cos\theta_{\hat{k}_{12},\hat{k}_3}\Big]\,,\end{aligned} \tag{4.6}$$

where $\hat{k}_{12}$ is the unit vector in the direction of $\mathbf{k}_1+\mathbf{k}_2$. We note that the unit-vector $\hat{k}_{12}$ enters in this expression, even though the corresponding vector $\vec{k}_1+\vec{k}_2$ vanishes in the squeezed limit (analogously to the $\hat{k}_3$-dependence of the bispectrum).

We observe that, in the $I^2(\phi)F^2$ model, both $f_{NL}^{\rm eff}$ and $\tau_{NL}^{\rm eff}$ exhibit highly non-trivial momentum dependence; thus, it is not sensible to compare different configurations. One can readily see that $\tau_{\rm NL}^{\rm eff}$ vanishes for several configurations. This happens, for example, if one of $\hat{k}_1\,,\hat{k}_{12}\,,\hat{k}_3$ is parallel to $\hat{E}_{\rm cl}$, while the other two vectors are perpendicular to $\hat{E}_{\rm cl}$. We do not interpret this as a violation of the Suyama-Yamaguchi inequality; the expression given by Eq. (4.4) requires either that the non-linearity parameters are momentum-independent, or else that $\tau_{NL}^{\rm eff}$ and $\left(f_{NL}^{\rm eff}\right)^2$ have the same momentum dependence so that one can factor out an amplitude which obeys Eq. (4.4). The original form of the Suyama-Yamaguchi inequality is simply not applicable to the model given by Eq. (2.7).[11]

In Ref. [21] Assassi et al derived a general inequality relating the soft limits of the bispectrum and trispectrum:

$$\int d^3q_1 d^3q_2\ \tau_{NL}^{\rm eff}(\mathbf{q}_1,\mathbf{k}-\mathbf{q}_1,\mathbf{q}_2,-\mathbf{q}_2-\mathbf{k})\ P_\zeta(q_1)P_\zeta(q_2)$$
$$\geq \left[\int d^3q\ \frac{6}{5}\,f_{NL}^{\rm eff}(\mathbf{q},-\mathbf{q}-\mathbf{k},\mathbf{k})\ P_\zeta(q)\right]^2\,, \tag{4.7}$$

where the $k\to 0$ limit is understood. This inequality reduces to Eq. (4.4) in the local case, but is completely general and should be respected by *any* model. We can easily verify that, although the Suyama-Yamaguchi inequality is not meaningful here, Eq. (4.7) is still respected. After evaluating the angular integral, the left hand side of Eq. (4.7) becomes

$$\text{LHS}\simeq 1024\pi^2\frac{24E_{\rm cl}^2}{\epsilon V(\phi)}\sin^2\theta_{\hat{k},\,\hat{E}_{\rm cl}}\left(\int dq\,q^2N_qP_\zeta\,(q)\right)^2\,, \tag{4.8}$$

and, proceeding analogously, the right hand side becomes

$$\text{RHS}\simeq 1024\pi^2N_k^2\left[\frac{24E_{\rm cl}^2}{\epsilon V(\phi)}\right]^2\sin^4\theta_{\hat{k},\,\hat{E}_{\rm cl}}\left(\int dq\,q^2N_qP_\zeta\,(q)\right)^2\,. \tag{4.9}$$

Therefore, we find

$$\frac{\text{LHS}}{\text{RHS}}\simeq\frac{1}{|g_*\,(N_k)\,|\sin^2\theta_{\hat{k},\,\hat{E}_{\rm cl}}}>1. \tag{4.10}$$

Note that $|g_*|\ll 1$ has been assumed (as also required by phenomenology) throughout this subsection. We therefore conclude that the integrated inequality given by Eq. (4.7) is satisfied for any orientations of $\vec{k}$ relative to the classical vector field background.

[11] Ref. [94] presents a detailed discussion on how to generalize the Suyama-Yamaguchi inequality to momentum-dependent non-linearity parameters, with a particular emphasis on the case of broken statistical isotropy. The fact that we have shown that there exist some configurations with vanishing $\tau_{NL}^{\rm eff}$ implies that, at least in principle, one may obtain observational evidence for a smaller squeezed trispectrum than the one obtained from scalar fields, provided that one can construct an observable quantity which is sensitive to those configurations. It remains to be seen whether such a measurement is feasible.

5 Conclusion

The angle dependence of the bispectrum of primordial curvature perturbations in the squeezed configuration is sensitive to the presence of vector fields and non-trivial symmetry during inflation. In this paper, we have explored phenomenological consequences of the new parametrization of the bispectrum given by Eq. (1.1): $B_\zeta = \sum_L c_L P_L(\hat{\mathbf{k}}_1 \cdot \hat{\mathbf{k}}_2) P_\zeta(k_1) P_\zeta(k_2) +$ (2 perm). This form is physically well motivated, and we have given three examples in Sec. 2: the curvature perturbation sourced by the anisotropic stress of magnetic fields; that sourced by an interaction with a vector field of the form $I^2(\phi)F^2$; and solid inflation.

We find that a cosmic-variance-limited CMB experiment measuring temperature anisotropy up to $\ell_{\rm max} = 2000$, such as the *Planck* satellite, can measure c_1 and c_2 down to $\delta c_1 = 61$ and $\delta c_2 = 13$ (68% CL). The latter error bar is comparable to (and only a factor of three larger than) the error bar of $c_0 = 6 f_{\rm NL}/5$; thus, if the forthcoming *Planck* data reveal evidence for c_0, one should also measure c_2 to understand the nature of sources of non-Gaussianity. Moreover, even if the *Planck* data do not reveal evidence for c_0, one should still measure c_2, as solid inflation can generate large c_2 *without generating detectable* c_0. Sensitivity to c_1 is an order of magnitude worse than that to c_0 or c_2 because the term proportional to c_1 vanishes in the squeezed limit due to symmetry.

The angle-dependent bispectrum in the squeezed configuration is a natural consequence of broken statistical isotropy. Broken isotropy also leads to a non-trivial modification of the inequality between the local-form trispectrum amplitude, $\tau_{\rm NL}$, and $f_{\rm NL}^2$. We find that the original form of the Suyama-Yamaguchi inequality, $\tau_{\rm NL} \geq (6 f_{\rm NL}/5)^2$, does not apply to the current model, due to the momentum- and shape-dependence of $\tau_{\rm NL}$ and $f_{\rm NL}$. For example, we find some squeezed configurations in which $\tau_{\rm NL}$ vanishes. It remains to be seen how sensitive the forthcoming tests of the Suyama-Yamaguchi inequality using the *Planck* or the large-scale structure data are to the decrease of the trispectrum amplitudes for these particular shapes. We also find that a general inequality of Ref. [21] is satisfied in this model.

What is next? Phenomenological consequences of Eq. (1.1) for large-scale structure of the universe such as the dark matter halo bias [95], bispectrum, and trispectrum should certainly be explored. For instance, a consistency relation [96, 97] between the squeezed bispectrum and the power spectrum of dark matter density fluctuations has been proved at the full nonlinear level, and with an initial isotropic non-Gaussianity, in [96]. It may be interesting to study a signature of anisotropic initial non-Gaussianity in that context. Also, it is quite possible that the coefficients c_L depend on wavenumbers, which would be particularly interesting for dipolar and quadrupolar modulations of the observed power spectrum in our sky [33]. Indeed, in the case of the $I^2(\phi)F^2$ model discussed in Sec. 2.2, the c_L coefficients exhibit a logarithmic running with wavenumber. It would be interesting to study possible effects of such wavenumber dependence.

Acknowledgments

MP and EK thank Kavli Institute for the Physics and Mathematics of the Universe (Kavli IPMU, WPI), where this work was initiated, for hospitality during our stay. MS and EK thank the organizers of the Long-term Workshop YITP-T-12-03 on "Gravity and Cosmology 2012" held at the Yukawa Institute for Theoretical Physics, Kyoto University, during which the initial draft of this paper was written. This work was supported in part by a Grant-in-Aid for JSPS Research under Grant No. 22-7477 (MS), and Grant-in-Aid for Nagoya University

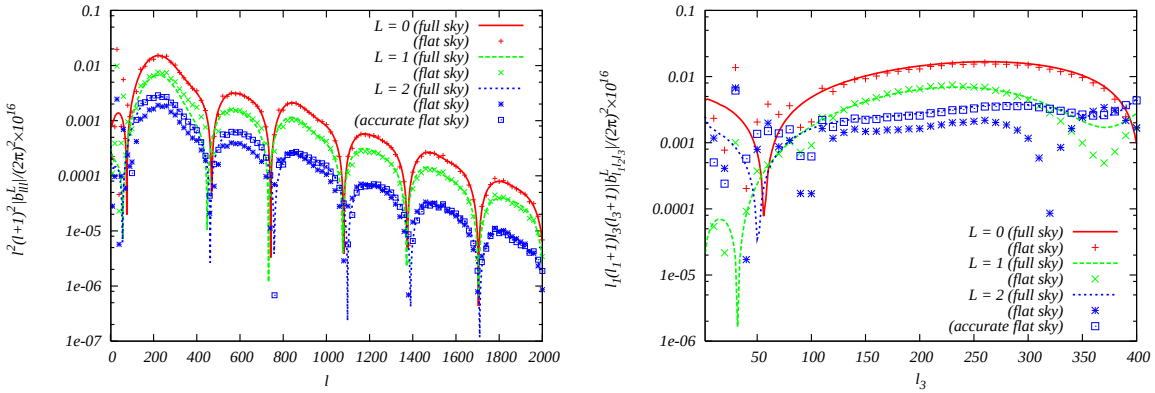

Figure 5. Absolute values of the CMB temperature reduced bispectra. The solid, long-dashed and short-dashed lines show the full-sky results for $L = 0$, 1, and 2, respectively, while the plus, cross, and star symbols show the simplified flat-sky results from Eq. (3.8) for $L = 0$, 1, and 2, respectively. The square symbols show the original form of the flat-sky result for $L = 2$ from Eq. (3.3) before further approximation. (Left panel) Equilateral triangles, $|b^L_{\ell\ell\ell}|$. (Right panel) Squeezed triangles, $|b^L_{\ell_1\ell_2\ell_3}|$, with $\ell_1 = \ell_2 = 200$, as a function of ℓ_3.

Global COE Program "Quest for Fundamental Principles in the Universe: from Particles to the Solar System and the Cosmos," from the Ministry of Education, Culture, Sports, Science and Technology of Japan. We also acknowledge the Kobayashi-Maskawa Institute for the Origin of Particles and the Universe, Nagoya University, for providing computing resources. MP thanks Nicola Bartolo and Sabino Matarrese for valuable discussions. NB and MP acknowledge partial support from the DOE grant DE-FG02-94ER-40823 at the University of Minnesota. MP would like to thank the University of Padova, and INFN, Sezione di Padova, for their friendly hospitality and for partial support during his sabbatical leave. NB is grateful to Valentin Assassi and Daniel Baumann for interesting discussions.

A Precision of the flat-sky approximation

How precise are the flat-sky formulae given by Eqs. (3.3) and (3.8)? In Figure 5, we compare the full-sky results with the flat-sky results. We find that, for $L = 0$ and 1, the simplified flat-sky formula given by Eq. (3.8) yields the bispectra in the equilateral and squeezed configurations which are in good agreement with the full-sky results at $\ell \gtrsim 100$. However, we find that, for $L = 2$, the simplified formula systematically underestimate the magnitude of the bispectra in both configurations. The equilateral result suggests that the simplified formula provides an adequate result only at $\ell \gtrsim 800$.

While these results appear to suggest that the precision of the simplified formula degrades as L increases, this is not the case: the flat-sky results in the Sachs-Wolfe limit (which are not shown in this paper) show that the simplified formula *overestimates* the magnitudes of the bispectra of $L = 1$ and 2 in the Sachs–Wolfe limit by a similar amount in both equilateral and squeezed configurations. Therefore, we conclude that the simplified formula given by Eq. (3.8) should only be used for quantitative calculations of $L = 0$ or for *qualitative* calculations of $L = 1$ and 2, and the original formula given by Eq. (3.3) should be used for quantitative calculations of $L = 1$ and 2. Needless to say, the full-sky formula should always be used for the calculations involving multipoles of $\ell \lesssim 100$.

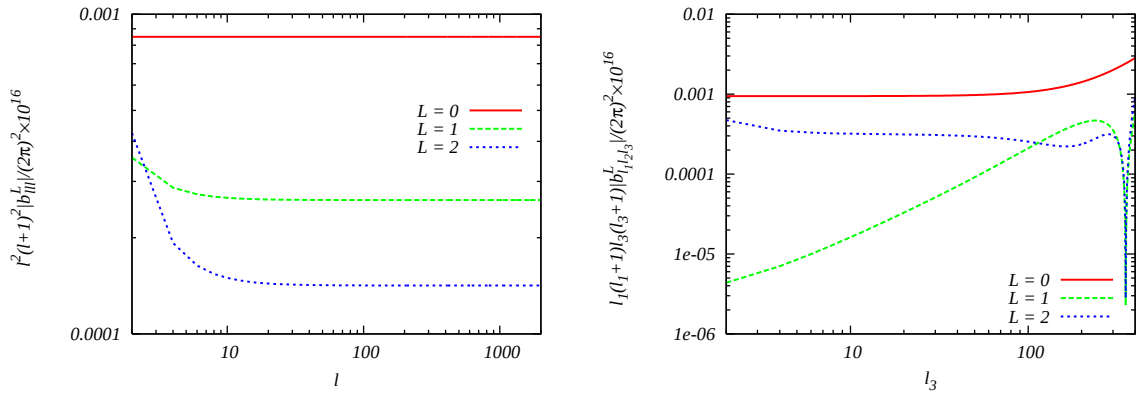

Figure 6. Absolute values of the CMB temperature reduced bispectra for $L = 0$ (solid), 1 (long-dashed), and 2 (short-dashed), in the Sachs–Wolfe limit. (Left panel) Equilateral triangles, $|b^L_{\ell\ell\ell}|$. (Right panel) Squeezed triangles, $|b^L_{\ell_1\ell_2\ell_3}|$, with $\ell_1 = \ell_2 = 200$, as a function of ℓ_3.

B Analysis in the Sachs-Wolfe limit

As the calculations presented in Sec. 3.2 are quite involved, some appropriate approximations would be useful for understanding the analytical structures of the basic results.

The Sachs–Wolfe limit, in which the radiation transfer function is given by $\mathcal{T}_\ell(k) \to -\frac{1}{5} j_\ell(kr_*)$, provides such a convenient approximation. With this transfer function, $\alpha_\ell(r)$ (Eq. 3.19) simplifies to $\alpha_\ell(r) \to -\frac{1}{5r_*^2}\delta(r - r_*)$, where $r_* \equiv \tau_0 - \tau_*$ is the conformal distance to the last scattering surface. Similarly, for a scale-invariant spectrum of ζ, $P_\zeta(k) = \frac{2\pi^2}{k^3} A_S$, $\beta_\ell(r)$ (Eq. 3.20) becomes

$$\beta_{\ell L}(r_*) \to -\frac{\pi^2}{10} A_S \frac{\Gamma\left(\frac{\ell+L}{2}\right)}{\Gamma\left(\frac{\ell-L+3}{2}\right)\Gamma\left(\frac{-\ell+L+3}{2}\right)\Gamma\left(\frac{\ell+L+4}{2}\right)} , \tag{B.1}$$

where $\Gamma(x)$ is the Gamma function. Using these α_ℓ and β_ℓ in Eq. (3.18), one finds the Sachs–Wolfe approximation of the CMB bispectrum as

$$\begin{aligned} B^L_{\ell_1\ell_2\ell_3} \to & -\frac{1}{5}\left[\prod_{n=1}^{3}\sum_{L_n}(-1)^{\frac{\ell_n+L_n}{2}}\right] I_{L_1L_2L_3}\beta_{\ell_1L_1}(r_*)\beta_{\ell_2L_2}(r_*) \\ & \times \frac{4\pi}{2L+1} I_{\ell_1L_1L} I_{\ell_2L_2L}(-1)^{\ell_2+L_1}\delta_{L_3,\ell_3}\begin{Bmatrix} \ell_1 & \ell_2 & \ell_3 \\ L_2 & L_1 & L \end{Bmatrix} + (2\ \text{perm}). \end{aligned} \tag{B.2}$$

Figure 6 shows the reduced CMB temperature bispectra in the Sachs–Wolfe limit. The basic behaviors, such as the monotonic decrease of the equilateral amplitudes as a function of L and the suppression of the $L = 1$ term in the squeezed limit, are all reproduced by the simple Sachs–Wolfe limit calculations. These results may be compared with Figures 2 and 3.

C Full Fisher matrix

In Sec. 3.3, we have presented the 1-σ marginalized constraints on c_0, c_1, and c_2, assuming that only c_0 and one of c_1 and c_2 are varied simultaneously. In this Appendix, we provide

the full Fisher matrix, $F_{LL'}$, involving all of c_0, c_1, and c_2, calculated up to $\ell_{\rm max} = 2000$:

$$F_{LL'} = \begin{pmatrix} 5232 & 16.94 & -5.986 \\ 16.94 & 26.53 & 66.85 \\ -5.986 & 66.85 & 618.1 \end{pmatrix} \times 10^{-5} \ . \tag{C.1}$$

From this matrix, one can compute the cross-correlation coefficients, $r_{LL'} \equiv F_{LL'}/\sqrt{F_{LL}F_{L'L'}}$. We find $r_{01} = 0.045$ and $r_{02} = -0.003$, indicating that c_0 and c_1 are nearly uncorrelated, so are c_0 and c_2. However, there is a high degree of correlation between c_1 and c_2: $r_{12} = 0.522$. As a result, the marginalized error bars increase slightly to

$$(\delta c_0, \delta c_1, \delta c_2) = \left(\sqrt{F_{00}^{-1}}, \sqrt{F_{11}^{-1}}, \sqrt{F_{22}^{-1}}\right) = (4.4, 72, 15) \ . \tag{C.2}$$

References

[1] P. Creminelli and M. Zaldarriaga, *Single field consistency relation for the 3-point function*, *JCAP* **0410** (2004) 006, [astro-ph/0407059].

[2] E. Komatsu, N. Afshordi, N. Bartolo, D. Baumann, J. Bond, *et. al.*, *Non-Gaussianity as a Probe of the Physics of the Primordial Universe and the Astrophysics of the Low Redshift Universe*, arXiv:0902.4759.

[3] I. Agullo and L. Parker, *Non-gaussianities and the Stimulated creation of quanta in the inflationary universe*, *Phys.Rev.* **D83** (2011) 063526, [arXiv:1010.5766].

[4] J. Ganc, *Calculating the local-type f_{NL} for slow-roll inflation with a non-vacuum initial state*, *Phys.Rev.* **D84** (2011) 063514, [arXiv:1104.0244].

[5] M. H. Namjoo, H. Firouzjahi, and M. Sasaki, *Violation of non-Gaussianity consistency relation in a single field inflationary model*, arXiv:1210.3692.

[6] X. Chen, H. Firouzjahi, M. H. Namjoo, and M. Sasaki, *A Single Field Inflation Model with Large Local Non-Gaussianity*, arXiv:1301.5699.

[7] E. Komatsu and D. N. Spergel, *Acoustic signatures in the primary microwave background bispectrum*, *Phys.Rev.* **D63** (2001) 063002, [astro-ph/0005036].

[8] G. Hinshaw, D. Larson, E. Komatsu, D. Spergel, C. Bennett, *et. al.*, *Nine-Year Wilkinson Microwave Anisotropy Probe (WMAP) Observations: Cosmological Parameter Results*, arXiv:1212.5226.

[9] Z. Hou, C. Reichardt, K. Story, B. Follin, R. Keisler, *et. al.*, *Constraints on Cosmology from the Cosmic Microwave Background Power Spectrum of the 2500-square degree SPT-SZ Survey*, arXiv:1212.6267.

[10] J. L. Sievers, R. A. Hlozek, M. R. Nolta, V. Acquaviva, G. E. Addison, *et. al.*, *The Atacama Cosmology Telescope: Cosmological parameters from three seasons of data*, arXiv:1301.0824.

[11] D. Babich, P. Creminelli, and M. Zaldarriaga, *The Shape of non-Gaussianities*, *JCAP* **0408** (2004) 009, [astro-ph/0405356].

[12] J. M. Maldacena, *Non-Gaussian features of primordial fluctuations in single field inflationary models*, *JHEP* **0305** (2003) 013, [astro-ph/0210603].

[13] C. Bennett, D. Larson, J. Weiland, N. Jarosik, G. Hinshaw, *et. al.*, *Nine-Year Wilkinson Microwave Anisotropy Probe (WMAP) Observations: Final Maps and Results*, arXiv:1212.5225.

[14] T. Okamoto and W. Hu, *The angular trispectra of CMB temperature and polarization*, *Phys.Rev.* **D66** (2002) 063008, [astro-ph/0206155].

[15] N. Kogo and E. Komatsu, *Angular trispectrum of cmb temperature anisotropy from primordial non-gaussianity with the full radiation transfer function*, *Phys.Rev.* **D73** (2006) 083007, [astro-ph/0602099].

[16] T. Suyama and M. Yamaguchi, *Non-Gaussianity in the modulated reheating scenario*, *Phys.Rev.* **D77** (2008) 023505, [arXiv:0709.2545].

[17] E. Komatsu, *Hunting for Primordial Non-Gaussianity in the Cosmic Microwave Background*, *Class.Quant.Grav.* **27** (2010) 124010, [arXiv:1003.6097].

[18] N. S. Sugiyama, E. Komatsu, and T. Futamase, *Non-Gaussianity Consistency Relation for Multi-field Inflation*, *Phys.Rev.Lett.* **106** (2011) 251301, [arXiv:1101.3636].

[19] K. M. Smith, M. LoVerde, and M. Zaldarriaga, *A universal bound on N-point correlations from inflation*, *Phys.Rev.Lett.* **107** (2011) 191301, [arXiv:1108.1805].

[20] N. S. Sugiyama, *Consistency Relation for multifield inflation scenario with all loop contributions*, *JCAP* **1205** (2012) 032, [arXiv:1201.4048].

[21] V. Assassi, D. Baumann, and D. Green, *On Soft Limits of Inflationary Correlation Functions*, *JCAP* **1211** (2012) 047, [arXiv:1204.4207].

[22] M. Shiraishi, D. Nitta, S. Yokoyama, and K. Ichiki, *Optimal limits on primordial magnetic fields from CMB temperature bispectrum of passive modes*, *JCAP* **1203** (2012) 041, [arXiv:1201.0376].

[23] M. Shiraishi, *Parity violation of primordial magnetic fields in the CMB bispectrum*, *JCAP* **1206** (2012) 015, [arXiv:1202.2847].

[24] N. Barnaby, R. Namba, and M. Peloso, *Observable non-gaussianity from gauge field production in slow roll inflation, and a challenging connection with magnetogenesis*, *Phys.Rev.* **D85** (2012) 123523, [arXiv:1202.1469].

[25] N. Bartolo, S. Matarrese, M. Peloso, and A. Ricciardone, *The anisotropic power spectrum and bispectrum in the $f(\phi)F^2$ mechanism*, arXiv:1210.3257.

[26] S. Endlich, A. Nicolis, and J. Wang, *Solid Inflation*, arXiv:1210.0569.

[27] M. Liguori, F. Hansen, E. Komatsu, S. Matarrese, and A. Riotto, *Testing primordial non-gaussianity in cmb anisotropies*, *Phys.Rev.* **D73** (2006) 043505, [astro-ph/0509098].

[28] C. T. Byrnes, S. Nurmi, G. Tasinato, and D. Wands, *Scale dependence of local f_{NL}*, *JCAP* **1002** (2010) 034, [arXiv:0911.2780].

[29] C. T. Byrnes, M. Gerstenlauer, S. Nurmi, G. Tasinato, and D. Wands, *Scale-dependent non-Gaussianity probes inflationary physics*, *JCAP* **1010** (2010) 004, [arXiv:1007.4277].

[30] S. Shandera, N. Dalal, and D. Huterer, *A generalized local ansatz and its effect on halo bias*, *JCAP* **1103** (2011) 017, [arXiv:1010.3722].

[31] J. Ganc and E. Komatsu, *Scale-dependent bias of galaxies and mu-type distortion of the cosmic microwave background spectrum from single-field inflation with a modified initial state*, *Phys.Rev.* **D86** (2012) 023518, [arXiv:1204.4241].

[32] I. Agullo and S. Shandera, *Large non-Gaussian Halo Bias from Single Field Inflation*, *JCAP* **1209** (2012) 007, [arXiv:1204.4409].

[33] F. Schmidt and L. Hui, *Cosmic Microwave Background Power Asymmetry from Non-Gaussian Modulation*, *Phys.Rev.Lett.* **110** (2013) 011301.

[34] P. Kronberg, M. Bernet, F. Miniati, S. Lilly, M. Short, *et. al.*, *A Global Probe of Cosmic Magnetic Fields to High Redshifts*, *Astrophys.J.* **676** (2008) 7079, [arXiv:0712.0435].

[35] M. L. Bernet, F. Miniati, S. J. Lilly, P. P. Kronberg, and M. Dessauges-Zavadsky, *Strong magnetic fields in normal galaxies at high redshifts*, *Nature* **454** (2008) 302–304,

[arXiv:0807.3347].

[36] A. M. Wolfe, R. A. Jorgenson, T. Robishaw, C. Heiles, and J. X. Prochaska, *An 84 microGauss Magnetic Field in a Galaxy at Redshift z=0.692*, *Nature* **455** (2008) 638, [arXiv:0811.2408].

[37] A. Fletcher, R. Beck, A. Shukurov, E. Berkhuijsen, and C. Horellou, *Magnetic fields and spiral arms in the galaxy M51*, arXiv:1001.5230.

[38] A. Neronov and I. Vovk, *Evidence for strong extragalactic magnetic fields from Fermi observations of TeV blazars*, *Science* **328** (2010) 73–75, [arXiv:1006.3504].

[39] K. Dolag, M. Kachelriess, S. Ostapchenko, and R. Tomas, *Lower limit on the strength and filling factor of extragalactic magnetic fields*, *Astrophys.J.* **727** (2011) L4, [arXiv:1009.1782].

[40] F. Tavecchio, G. Ghisellini, L. Foschini, G. Bonnoli, G. Ghirlanda, *et. al.*, *The intergalactic magnetic field constrained by Fermi/LAT observations of the TeV blazar 1ES 0229+200*, *Mon.Not.Roy.Astron.Soc.* **406** (2010) L70–L74, [arXiv:1004.1329].

[41] K. Takahashi, M. Mori, K. Ichiki, and S. Inoue, *Lower Bounds on Intergalactic Magnetic Fields from Simultaneously Observed GeV-TeV Light Curves of the Blazar Mrk 501*, arXiv:1103.3835.

[42] S. Kanno, J. Soda, and M.-a. Watanabe, *Cosmological Magnetic Fields from Inflation and Backreaction*, *JCAP* **0912** (2009) 009, [arXiv:0908.3509].

[43] V. Demozzi, V. Mukhanov, and H. Rubinstein, *Magnetic fields from inflation?*, *JCAP* **0908** (2009) 025, [arXiv:0907.1030].

[44] V. Demozzi and C. Ringeval, *Reheating constraints in inflationary magnetogenesis*, *JCAP* **1205** (2012) 009, [arXiv:1202.3022].

[45] T. Suyama and J. Yokoyama, *Metric perturbation from inflationary magnetic field and generic bound on inflation models*, *Phys.Rev.* **D86** (2012) 023512, [arXiv:1204.3976].

[46] T. Fujita and S. Mukohyama, *Universal upper limit on inflation energy scale from cosmic magnetic field*, *JCAP* **1210** (2012) 034, [arXiv:1205.5031].

[47] R. Durrer, T. Kahniashvili, and A. Yates, *Microwave background anisotropies from Alfven waves*, *Phys.Rev.* **D58** (1998) 123004, [astro-ph/9807089].

[48] A. Mack, T. Kahniashvili, and A. Kosowsky, *Microwave background signatures of a primordial stochastic magnetic field*, *Phys.Rev.* **D65** (2002) 123004, [astro-ph/0105504].

[49] A. Lewis, *CMB anisotropies from primordial inhomogeneous magnetic fields*, *Phys.Rev.* **D70** (2004) 043011, [astro-ph/0406096].

[50] D. G. Yamazaki, K. Ichiki, T. Kajino, and G. J. Mathews, *Effects of a Primordial Magnetic Field on Low and High Multipoles of the CMB*, *Phys.Rev.* **D77** (2008) 043005, [arXiv:0801.2572].

[51] D. Paoletti, F. Finelli, and F. Paci, *The full contribution of a stochastic background of magnetic fields to CMB anisotropies*, *Mon.Not.Roy.Astron.Soc.* **396** (2009) 523–534, [arXiv:0811.0230].

[52] F. Finelli, F. Paci, and D. Paoletti, *The Impact of Stochastic Primordial Magnetic Fields on the Scalar Contribution to Cosmic Microwave Background Anisotropies*, *Phys.Rev.* **D78** (2008) 023510, [arXiv:0803.1246].

[53] J. R. Shaw and A. Lewis, *Massive Neutrinos and Magnetic Fields in the Early Universe*, *Phys.Rev.* **D81** (2010) 043517, [arXiv:0911.2714].

[54] J. R. Shaw and A. Lewis, *Constraining Primordial Magnetism*, *Phys.Rev.* **D86** (2012) 043510, [arXiv:1006.4242].

[55] D. Paoletti and F. Finelli, *CMB Constraints on a Stochastic Background of Primordial Magnetic Fields*, *Phys.Rev.* **D83** (2011) 123533, [arXiv:1005.0148].

[56] D. Paoletti and F. Finelli, *Constraints on a Stochastic Background of Primordial Magnetic Fields with WMAP and South Pole Telescope data*, arXiv:1208.2625.

[57] A. P. Yadav, L. Pogosian, and T. Vachaspati, *Probing Primordial Magnetism with Off-Diagonal Correlators of CMB Polarization*, arXiv:1207.3356.

[58] M. Shiraishi, S. Saga, and S. Yokoyama, *CMB power spectra induced by primordial cross-bispectra between metric perturbations and vector fields*, *JCAP* **1211** (2012) 046, [arXiv:1209.3384].

[59] K. E. Kunze, *Cross correlations from back reaction on stochastic magnetic fields*, *JCAP* **1302** (2013) 009, [arXiv:1209.4570].

[60] K. E. Kunze, *CMB and matter power spectra from cross correlations of primordial curvature and magnetic fields*, arXiv:1301.6105.

[61] T. Seshadri and K. Subramanian, *CMB bispectrum from primordial magnetic fields on large angular scales*, *Phys.Rev.Lett.* **103** (2009) 081303, [arXiv:0902.4066].

[62] C. Caprini, F. Finelli, D. Paoletti, and A. Riotto, *The cosmic microwave background temperature bispectrum from scalar perturbations induced by primordial magnetic fields*, *JCAP* **0906** (2009) 021, [arXiv:0903.1420].

[63] P. Trivedi, K. Subramanian, and T. Seshadri, *Primordial Magnetic Field Limits from Cosmic Microwave Background Bispectrum of Magnetic Passive Scalar Modes*, *Phys.Rev.* **D82** (2010) 123006, [arXiv:1009.2724].

[64] R.-G. Cai, B. Hu, and H.-B. Zhang, *Acoustic signatures in the Cosmic Microwave Background bispectrum from primordial magnetic fields*, *JCAP* **1008** (2010) 025, [arXiv:1006.2985].

[65] M. Shiraishi, D. Nitta, S. Yokoyama, K. Ichiki, and K. Takahashi, *Cosmic microwave background bispectrum of vector modes induced from primordial magnetic fields*, *Phys.Rev.* **D82** (2010) 121302, [arXiv:1009.3632].

[66] M. Shiraishi, D. Nitta, S. Yokoyama, K. Ichiki, and K. Takahashi, *Computation approach for CMB bispectrum from primordial magnetic fields*, *Phys.Rev.* **D83** (2011) 123523, [arXiv:1101.5287].

[67] M. Shiraishi, D. Nitta, S. Yokoyama, K. Ichiki, and K. Takahashi, *Cosmic microwave background bispectrum of tensor passive modes induced from primordial magnetic fields*, *Phys.Rev.* **D83** (2011) 123003, [arXiv:1103.4103].

[68] C. Caprini, R. Durrer, and T. Kahniashvili, *The Cosmic microwave background and helical magnetic fields: The Tensor mode*, *Phys.Rev.* **D69** (2004) 063006, [astro-ph/0304556].

[69] M. Shiraishi, D. Nitta, and S. Yokoyama, *Parity Violation of Gravitons in the CMB Bispectrum*, *Prog.Theor.Phys.* **126** (2011) 937–959, [arXiv:1108.0175].

[70] A. R. Pullen and M. Kamionkowski, *Cosmic Microwave Background Statistics for a Direction-Dependent Primordial Power Spectrum*, *Phys.Rev.* **D76** (2007) 103529, [arXiv:0709.1144].

[71] Y.-Z. Ma, G. Efstathiou, and A. Challinor, *Testing a direction-dependent primordial power spectrum with observations of the Cosmic Microwave Background*, *Phys.Rev.* **D83** (2011) 083005, [arXiv:1102.4961].

[72] B. Ratra, *Cosmological 'seed' magnetic field from inflation*, *Astrophys.J.* **391** (1992) L1–L4.

[73] J. Martin and J. Yokoyama, *Generation of Large-Scale Magnetic Fields in Single-Field Inflation*, *JCAP* **0801** (2008) 025, [arXiv:0711.4307].

[74] R. R. Caldwell, L. Motta, and M. Kamionkowski, *Correlation of inflation-produced magnetic fields with scalar fluctuations*, *Phys.Rev.* **D84** (2011) 123525, [arXiv:1109.4415].

[75] L. Motta and R. R. Caldwell, *Non-Gaussian features of primordial magnetic fields in power-law inflation*, *Phys.Rev.* **D85** (2012) 103532, [arXiv:1203.1033].

[76] R. K. Jain and M. S. Sloth, *A Magnetic Consistency Relation*, arXiv:1207.4187.

[77] R. K. Jain and M. S. Sloth, *On the non-Gaussian correlation of the primordial curvature perturbation with vector fields*, arXiv:1210.3461.

[78] D. Seery, *Magnetogenesis and the primordial non-gaussianity*, *JCAP* **0908** (2009) 018, [arXiv:0810.1617].

[79] A. A. Starobinsky, *Stochastic De Sitter (inflationary) Stage In The Early Universe*, *Field heory, Quantum Gravity and Strings* (1986) 107–126.

[80] I. Affleck and M. Dine, *A New Mechanism for Baryogenesis*, *Nucl.Phys.* **B249** (1985) 361.

[81] D. H. Lyth and D. Wands, *Generating the curvature perturbation without an inflaton*, *Phys.Lett.* **B524** (2002) 5–14, [hep-ph/0110002].

[82] T. R. Dulaney and M. I. Gresham, *Primordial Power Spectra from Anisotropic Inflation*, *Phys.Rev.* **D81** (2010) 103532, [arXiv:1001.2301].

[83] A. Gumrukcuoglu, B. Himmetoglu, and M. Peloso, *Scalar-Scalar, Scalar-Tensor, and Tensor-Tensor Correlators from Anisotropic Inflation*, *Phys.Rev.* **D81** (2010) 063528, [arXiv:1001.4088].

[84] M.-a. Watanabe, S. Kanno, and J. Soda, *The Nature of Primordial Fluctuations from Anisotropic Inflation*, *Prog.Theor.Phys.* **123** (2010) 1041–1068, [arXiv:1003.0056].

[85] M.-a. Watanabe, S. Kanno, and J. Soda, *Inflationary Universe with Anisotropic Hair*, *Phys.Rev.Lett.* **102** (2009) 191302, [arXiv:0902.2833].

[86] R. Emami and H. Firouzjahi, *Curvature Perturbations in Anisotropic Inflation with Symmetry Breaking*, arXiv:1301.1219.

[87] K. Dimopoulos, M. Karciauskas, and J. M. Wagstaff, *Vector Curvaton without Instabilities*, *Phys.Lett.* **B683** (2010) 298–301, [arXiv:0909.0475].

[88] R. Namba, *Curvature Perturbations from a Massive Vector Curvaton*, *Phys.Rev.* **D86** (2012) 083518, [arXiv:1207.5547].

[89] H. Funakoshi and K. Yamamoto, *Primordial bispectrum from inflation with background gauge fields*, arXiv:1212.2615.

[90] S. Yokoyama and J. Soda, *Primordial statistical anisotropy generated at the end of inflation*, *JCAP* **0808** (2008) 005, [arXiv:0805.4265].

[91] A. Gruzinov, *Elastic inflation*, *Phys.Rev.* **D70** (2004) 063518, [astro-ph/0404548].

[92] M. Shiraishi, S. Yokoyama, K. Ichiki, and K. Takahashi, *Analytic formulae of the CMB bispectra generated from non-Gaussianity in the tensor and vector perturbations*, *Phys.Rev.* **D82** (2010) 103505, [arXiv:1003.2096].

[93] M. Shiraishi, D. Nitta, S. Yokoyama, K. Ichiki, and K. Takahashi, *CMB Bispectrum from Primordial Scalar, Vector and Tensor non-Gaussianities*, *Prog.Theor.Phys.* **125** (2011) 795–813, [arXiv:1012.1079].

[94] Y. Rodriguez, J. P. B. Almeida, and C. A. Valenzuela-Toledo, *The different varieties of the Suyama-Yamaguchi consistency relation and its violation as a signal of statistical inhomogeneity*, arXiv:1301.5843.

[95] M. Shiraishi, S. Yokoyama, K. Ichiki, and T. Matsubara, *Scale-dependent bias due to primordial vector field*, arXiv:1301.2778.

[96] M. Peloso and M. Pietroni, *Galilean invariance and the consistency relation for the nonlinear*

squeezed bispectrum of large scale structure, arXiv:1302.0223.

[97] A. Kehagias and A. Riotto, *Symmetries and Consistency Relations in the Large Scale Structure of the Universe*, arXiv:1302.0130.